Asymptotic Analysis of the Lattice Boltzmann Equation

Michael Junk[†], Axel Klar[‡], and Li-Shi Luo[*]

[†]*FB Mathematik und Statistik, Universität Konstanz, Fach D194,
78457 Konstanz, Germany*
[‡]*FB Mathematik, TU Kaiserslautern, 67663 Kaiserslautern, Germany*
[*]*Department of Mathematics and Statistics, Old Dominion University,
Norfolk, Virginia 23529, USA*

E-mail: `michael.junk@uni-konstanz.de`, `klar@mathematik.uni-kl.de`, `lluo@odu.edu`

In this article we analyze the lattice Boltzmann equation (LBE) by using the asymptotic expansion technique. We first relate the LBE to the finite discrete-velocity model (FDVM) of the Boltzmann equation with the diffusive scaling. The analysis of this model directly leads to the *incompressible* Navier-Stokes equations, as opposed to the *compressible* Navier-Stokes equations obtained by the Chapman-Enskog analysis with convective scaling. We also apply the asymptotic analysis directly to the fully discrete LBE, as opposed to the usual practice of analyzing a continuous equation obtained through the Taylor-expansion of the LBE. This leads to a consistency analysis which provides order-by-order information about the numerical solution of the LBE. The asymptotic technique enables us to analyze the structure of the leading order errors and the accuracy of numerically derived quantities, such as vorticity. It also justifies the use of Richardson's extrapolation method. As an example, a two-dimensional Taylor-vortex flow is used to validate our analysis. The numerical results agree very well with our analytic predictions.

1. INTRODUCTION

Historically the lattice Boltzmann equation (LBE) is originated from the lattice gas cellular automata (LGCA) [13, 12]. The lattice gas cellular automata represent an innovative and yet highly unconventional methodology to simulate physical systems which can or cannot be represented by partial differential equations (PDEs). The LGCA methodology is deemed appropriate in those areas where PDE is not an adequate description, *e.g.*, artificial life or language theory (cf. [22]). However,

1

in computational fluid dynamics (CFD), a well-established area in which the solutions of a set of PDEs — the Navier-Stokes equations — are the primary objective, the novel and unconventional LGCA methodology has met with severe criticisms because, not only is the method unconventional, but also it has not been systematically subjected to the rigorous (numerical) analysis like other conventional CFD methods based on discretizations of the Navier-Stokes equations. Apparently, the historic connection to LGCA is a factor hampering a wider acceptance of the lattice Boltzmann method (LBM), in spite of the evidence accumulated so far has shown that the method is not only valid, but also competitive in some circumstances (such as complex fluid flows through porous media (cf. [37]) and non-spherical particulate suspensions in fluid flows [40, 38, 39]). Nevertheless, similar to LGCA, questions concerning the consistency, stability, and convergence of LBM have been unanswered or answered unsatisfactorily.

In this article we intend to fill gaps the mathematical analysis of the lattice Boltzmann equation in the following two aspects. The first is to establish the direct connection between the lattice Boltzmann equation and the classical kinetic theory (without referring to LGCA). It can be demonstrated that the lattice Boltzmann equation is in fact a finite difference form of the finite discrete-velocity model of the Boltzmann equation in a particular scaling. And the second is to provide an asymptotic analysis of the lattice Boltzmann equation so that the mathematical properties (consistency) of the lattice Boltzmann method can be well illustrated.

An asymptotic expansion is a well established method in the theory of ordinary differential equations and is also frequently used for PDEs in connection with Richardson's extrapolation or deferred correction methods (cf. review in [26]). We shall demonstrate that the lattice Boltzmann method is by no means special as far as its analysis is concerned: it can be analyzed in the same fashion as other traditional numerical schemes, such as the schemes for the Laplace or heat equations [26]. In particular, we can obtain the spatial and temporal accuracy of the lattice Boltzmann equation, analyze the accuracy of quantities like vorticity which are not directly available as velocity moments, justify the use of extrapolation techniques, and gain accurate and quantitative information about the structure of the leading order error.

Classically, the Chapman-Enskog (CE) expansion is employed to analyze the consistency of LBE. Starting point for the CE analysis is the usual (convective) scaling, $i.e.$, $\Delta x \sim \Delta t$, which is subsequently combined with a two-timescale expansion to derive the hydrodynamic equations. The resulting macroscopic equations describe $compressible$ flows in the faster time scale and diffusive effects in the slower one. Eventually, the equations can be related to the compressible Navier-Stokes system from which the incompressible equations are obtained in another limiting process [12, 2, 6, 7, 18, 19, 47].

In contrast to this traditional approach, we advocate the $diffusive\ scaling$ as a mathematical alternative to analyze the lattice Boltzmann equation. The diffusive scaling, developed by Sone (cf. [43]), is well known in kinetic theory and has been used to establish a direct connection between the Boltzmann equation and the incompressible Navier-Stokes equations [9, 1, 29, 14, 15]. In particular, the diffusive scaling is the natural choice if the LBE is viewed purely as a numerical method to solve the $incompressible$ Navier-Stokes equation. In this case, compressibility effects

are considered as numerical effects and it suffices to consider the slower (diffusive) time scale in the analysis. Thus the technical advantages of the advocated method are twofold. First, only a single time scale expansion is necessary and it is simpler than a two-scale expansion because the expansion coefficients and the corresponding equations depend on one variable fewer. Second, the expansion coefficients depend directly on the aspired solution of the incompressible Navier-Stokes problem and not on the solution of a different problem (the compressible equation). Having this direct dependence, it is straight forward to relate the numerical solution to the exact solution, for example, to obtain error estimates.

An obvious difference between the classical Chapman-Enskog analysis and our approach here is the relation $\Delta t \sim \Delta x^2$ for the time step. This assumption is natural if we restrict ourselves to flows which are slow compared to the particle velocity defined in the LBE and which are interpreted in the slow (diffusive) time scale. Note, however, that the assumption does not alter the lattice Boltzmann algorithm. It is merely a different scaling which simplifies the analysis of the underlying LBE scheme. In order to make this point more precise, let us think of a flow through a channel of length L with typical velocity U. In the classical scaling (where $\Delta t \sim \Delta x$), U has to be a small quantity (of the order of Δx) which reflects the low Mach number assumption. In particular, the time required for a volume of fluid to traverse the channel is proportional to $L/U = \mathcal{O}(1/\Delta x)$ and thus diverges for $\Delta x \to 0$. With a time step $\Delta t \sim \Delta x$ in the simulation, a typical number of time steps required for this fluid displacement is $\mathcal{O}(1/\Delta x^2)$. In contrast to the classical scaling where flow speed and simulation time converge to zero and infinity, respectively, for $\Delta x \to 0$, we avoid technical difficulties by using a scaling in which the flow velocity U is of order one so that the macroscopic time L/U is also of order one. Due to the relation $\Delta t \sim \Delta x^2$, however, the required number of time steps is again of order $\mathcal{O}(1/\Delta x^2)$ reflecting the fact that the underlying lattice Boltzmann algorithm is unchanged.

With the exception of [23], the diffusive scaling has not been applied to analyze the lattice Boltzmann equation. However, it is important to emphasize that the our analysis differs from that in [23] because we do not approximate the *discrete* lattice Boltzmann equation with a continuous equation through Taylor expansion, as in [23]. In fact, the expansion used here implicitly assumes that the discrete solution can be obtained by restricting a smooth function to the grid which breaks down if the numerical solution exhibits initial or boundary layers. In the modified equation analysis, the same assumption is used and it has been shown, for example in [16, 5], that it lacks mathematical justification. Since our goal is to develop a method which will enable us to analyze the lattice Boltzmann method in combination with boundary conditions [25], coupling conditions for different meshes [42] and in the presence of initial layers [4], we circumvent this technical problem and apply an asymptotic expansion directly to the discrete lattice Boltzmann equation itself, in the spirit of [45, 46, 33].

We conclude the introduction with an outline of the article. In Sec. 2 we provide a concise account of the kinetic origin of the lattice Boltzmann equation. In Sec. 3 we introduce a coordinate-free notation and the assumptions on the structures of the discrete velocity set and the collision operator. We consider a very general situation including the models in two or three dimensions with multiple-relaxation-

time (MRT) collision operators [10], of which the Bhatnagar-Gross-Krook (BGK) [3] collision operator is merely a special case. In Sec. 4 we discuss the asymptotic analysis of the finite-discrete velocity model (with continuous space $\boldsymbol{x}$ and time t), which facilitates the analysis of the lattice Boltzmann equation. Details of the derivations are deferred to Appendix A. In Sec. 5, we present the asymptotic analysis of the lattice Boltzmann equation. We show that the lattice Boltzmann approximation to the *incompressible* Navier-Stokes equations is at least second-order accurate in space and first-order accurate in time. In Sec. 6 we consider in detail a rotating flow in two dimensions as a test case to verify our analysis. Finally, in Sec. 7 we summarize our results and conclude the paper. The Appendices contain the technical details of the asymptotic analysis and provides examples for lattice Boltzmann models which satisfy the assumptions of our general approach in Sec. 3.

2. KINETIC ORIGIN OF THE LATTICE BOLTZMANN EQUATION

We consider the finite discrete-velocity model (FDVM) of the Boltzmann equation with the finite discrete velocity set $\mathbb{V} = \{\boldsymbol{c}_0, \ldots, \boldsymbol{c}_N\}$:

$$\partial_t f_i + \boldsymbol{c}_i \cdot \boldsymbol{\nabla} f_i = J_i, \qquad i = 0, \ldots, N, \tag{1}$$

where the function $f_i(t, \boldsymbol{x}) = f(t, \boldsymbol{x}, \boldsymbol{c}_i)$ is the single particle (mass) density distribution function at time $t \in [0, T]$ and position $\boldsymbol{x} \in \Omega$. While the left hand side of Eq. (1) describes the transport of a particle, the right hand side describes the change of f_i due to collisional interactions among the particles. With the *diffusive scaling* $\boldsymbol{x} \to \boldsymbol{x}/\epsilon$ and $t \to t/\epsilon^2$, we concentrate on macroscopic processes (large space scale) over very long time intervals (slow time scale). Eq. (1) becomes

$$\epsilon^2 \partial_t f_i + \epsilon \boldsymbol{c}_i \cdot \boldsymbol{\nabla} f_i = J_i, \qquad i = 0, \ldots, N. \tag{2}$$

Dividing Eq. (2) by ϵ^2 and integrating it along characteristics, we obtain

$$f_i(t + \Delta t, \boldsymbol{x} + \boldsymbol{c}_i \Delta t/\epsilon) = f_i(t, \boldsymbol{x}) + \frac{1}{\epsilon^2} \int_0^{\Delta t} J_i(t + s, \boldsymbol{x} + \boldsymbol{c}_i s/\epsilon) \, ds.$$

By using the space and time step size according to the diffusive scaling $\Delta t = \epsilon^2$ and $\Delta x = \epsilon$, and approximating the integral by the rectangle rule with the integrand evaluated at the left point of the interval, we arrive at

$$f_i(t + \Delta t, \boldsymbol{x} + \boldsymbol{c}_i \Delta x) \approx f_i(t, \boldsymbol{x}) + J_i(t, \boldsymbol{x}). \tag{3}$$

We can transform Eq. (3) into a simple algorithm on a spatial lattice $\mathbb{X}$ which is invariant under $\boldsymbol{c}_i$-translations, *i.e.*,

$$\boldsymbol{c}_i + \mathbb{X} = \mathbb{X}, \qquad i = 0, \ldots, N.$$

If we use $\hat{f}_i(k, \boldsymbol{j})$, with $k \in \mathbb{N}_0 := \{0, 1, 2, \ldots\}$ and $\boldsymbol{j} \in \mathbb{X}$, to approximate the value $f_i(k\Delta t, \boldsymbol{j}\Delta x)$, then we obtain the lattice Boltzmann evolution using Eq. (3) [18, 19]:

$$\hat{f}_i(k + 1, \boldsymbol{j} + \boldsymbol{c}_i) = \hat{f}_i(k, \boldsymbol{j}) + \hat{J}_i(k, \boldsymbol{j}). \tag{4}$$

Of course, one could derive variants of the lattice Boltzmann equation by using different discretizations of Eq. (2) than those described above, but this is not our objective here. The point of this brief derivation is to demonstrates the explicit connection between the lattice Boltzmann equation (4) and the finite discrete-velocity model equation (1) with the diffusive scaling. Moreover, it already indicates a fundamental difficulty in the analysis: since the lattice Boltzmann equation (4) can be viewed as a discretization of the singularly perturbed FDVM equation (2) with coupled parameters $\Delta t = \Delta x^2 = \epsilon^2$, it is clear that, in the limit of $\epsilon \to 0$, Eq. (4) does not approximate the kinetic equation (1) from which it has been derived, because the structure of this equation changes qualitatively in the limit (in lowest order it reduces to an algebraic equation $J_i = 0$). Therefore, the analysis of the lattice Boltzmann equation (4) is inevitably related to the asymptotic analysis of Eq. (1) with appropriate scalings.

Usually, the Chapman-Enskog analysis combined with a Taylor expansion is used to analyze the lattice Boltzmann equation (4) and it is well known that the averaged particle velocity approximates solutions of the incompressible Navier-Stokes equation in a limit of low Mach number. In this article we would like to demonstrate that this result can also be obtained with a straightforward asymptotic expansion of Eq. (4). Similar expansions have been widely applied to numerical schemes for solving ordinary and partial differential equations, for example, to derive and improve the order of consistency. In particular, the asymptotic analysis also allows us to study an algorithm with boundary or coupling conditions, or initial layers. By embedding the analysis into a framework which is *generally* applicable to finite difference schemes, we hope to *clarify* and *improve* the numerical analysis of lattice Boltzmann method.

3. STRUCTURAL ASSUMPTIONS
3.1. Coordinate free notation

For the sake of concreteness and simplicity, we shall consider collision operators with a particular structure which may not contain all possible realizations of lattice Boltzmann models. Nevertheless, the techniques described here are fairly general. We should restrict ourselves to athermal LBE models (without energy conservation). We also stress that the notation to be used in what follows is coordinate free for velocity-dependent functions. If $\mathbb{V} = \{\boldsymbol{c}_0, \ldots, \boldsymbol{c}_N\} \subset \mathbb{R}^d$ is the set of d-dimensional discrete velocities, we introduce the Euclidean vector space $\mathcal{F}$ of real valued functions $f : \mathbb{V} \to \mathbb{R}$. Most of the lattice Boltzmann literature relies on the choice of a canonical basis in $\mathcal{F}$ given by the Kronecker functions $\delta_{\boldsymbol{c}_i} \in \mathcal{F}$, $\delta_{\boldsymbol{c}_i}(\boldsymbol{c}_j) = \delta_{ij}$. In this basis, a function $f \in \mathcal{F}$ has the representation

$$f(\boldsymbol{v}) = \sum_{i=0}^{N} f(\boldsymbol{c}_i)\delta_{\boldsymbol{c}_i}(\boldsymbol{v})$$

with coordinates $f_i = f(\boldsymbol{c}_i)$. Obviously, the formulation of the lattice Boltzmann equation (4) and its continuous counterpart (1) is based on these coordinates.

Another useful basis is given by polynomials $\{\phi_0, \ldots, \phi_N\} \subset \mathcal{F}$ which are, for example, orthogonal with respect to the standard scalar product on $\mathcal{F}$

$$\langle f, g \rangle = \sum_{i=0}^{N} f(\boldsymbol{c}_i) g(\boldsymbol{c}_i), \qquad f, g \in \mathcal{F}.$$

In this basis, a function f has the representation

$$f(\boldsymbol{v}) = \sum_{i=0}^{N} \langle f, \phi_i \rangle \, \phi_i(\boldsymbol{v}).$$

Now the coordinates are (velocity) moments of f. For example, $\phi_0(\boldsymbol{v}) = 1$ and $\phi_1(\boldsymbol{v}) = v_x$, then

$$\rho = \langle f, \phi_0 \rangle = \sum_{i=0}^{N} f(\boldsymbol{c}_i) \quad \text{and} \quad j_x = \langle f, \phi_1 \rangle = \sum_{i=0}^{N} f(\boldsymbol{c}_i) c_{ix}$$

are averaged mass density and x-momentum, respectively. Consequently, if the lattice Boltzmann evolution is formulated in a polynomial basis, one obtains equations for velocity moments — so called moment systems [10, 24]. However, to avoid an *a priori* choice for a particular basis, we use as much as possible a coordinate-free notation which has several advantages. First, coordinate-free notations emphasize the essentials. Second, this notation is so general that it is model-independent, thus the analysis clearly carries over to all models. And finally, the notation is compatible with continuous velocity sets $\mathbb{V}$ so that the connection to well established results in classic kinetic theory is immediate (only the scalar product $\langle \cdot, \cdot \rangle$ has to be replaced by the $\mathbb{L}^2$ scalar product).

To cast Eq. (2) in a coordinate-free notation, we introduce the velocity multiplication operators $V_\alpha : \mathcal{F} \to \mathcal{F}$ defined by $(V_\alpha f)(\boldsymbol{v}) = v_\alpha f(\boldsymbol{v})$, where the Greek subscripts α, β, $\ldots$, are always used to denote the Cartesian coordinates 1, $\ldots$, d as opposed to the Roman subscripts i, j, $\ldots$, labeling discrete velocities. Note that $V_\alpha 1$ is the function $\boldsymbol{v} \mapsto v_\alpha$. For abbreviation, we consider $\{V_\alpha | \alpha = 1, 2, \ldots, d\}$ as components of a vector operator $\mathbf{V} = (V_1, \ldots, V_d)^\mathsf{T}$, where the superscript T indicates the transpose operation. Equation (2) can be concisely written as an equation for the function $f : \mathbb{R}_0^+ \times \Omega \times \mathbb{V} \to \mathbb{R}$ defined by $f(t, \boldsymbol{x}, \boldsymbol{c}_i) := f_i(t, \boldsymbol{x})$

$$\partial_t f + \frac{1}{\epsilon} \mathbf{V} \cdot \boldsymbol{\nabla} f = \frac{1}{\epsilon^2} J(f). \tag{5}$$

As previously indicated, the above equation differs from the hydrodynamic scaling of the Boltzmann equation, in which the small parameter (the Knudsen number) ϵ only appears inversely in front of the collision term.

3.2. The collision operator and the equilibrium distribution

The collision operator $J : \mathcal{F} \to \mathcal{F}$ in (5) will be chosen of relaxation type

$$J(f) = \mathsf{A}[f^{(\mathrm{eq})}(f) - f],$$

where $\mathsf{A} : \mathcal{F} \to \mathcal{F}$ is a linear mapping, and $f^{(\mathrm{eq})} : \mathcal{F} \to \mathcal{F}$ is the so called equilibrium distribution. The idea to use collision operators of relaxation type in the

lattice Boltzmann equation was proposed in previous works [20, 21, 35, 10]. In the multiple-relaxation-time (MRT) or generalized lattice Boltzmann equation [10], the operator A is explicitly constructed with an orthonormal basis in $\mathcal{F}$ such that A is diagonalized in this basis. Obviously the MRT approach is more flexible in tuning some physical parameters (*e.g.*, Prandtl number Pr), and has been shown to be numerically more stable [28] than the popular lattice BGK collision operator [41, 6], of which A is a multiple of the identity operator. In what follows, we shall use the multiple-relaxation-time (linear) collision operator A which is essentially determined by certain algebraic properties reflecting the conservation laws and associated symmetries. To avoid restriction to any particular model, we shall prescribe the criteria on $f^{(\mathrm{eq})}$ and A which are necessary for the subsequent analysis. Examples for lattice Boltzmann models satisfying these assumptions are given in the Appendices.

The first assumption is that the velocity set $\mathbb{V}$ is symmetric, *i.e.*,

$$\mathbb{V} = -\mathbb{V} \tag{6}$$

which allows us to define even and odd functions (cf. Appendix A.1). We call a function even, if $f(-\boldsymbol{c}_i) = f(\boldsymbol{c}_i)$ and odd if $f(-\boldsymbol{c}_i) = -f(\boldsymbol{c}_i)$. Second, we assume the existence of an even function $f^* \in \mathcal{F}$ for which the lowest order moments have the same isotropy structure as the classical Maxwellian

$$M(\boldsymbol{v}) = \frac{1}{(2\pi\theta)^{\frac{d}{2}}} \exp\left(-\frac{\boldsymbol{v}^2}{2c_s^2}\right), \qquad \boldsymbol{v} \in \mathbb{R}^d,$$

where $\theta = c_s^2$ is the scaled temperature, and the parameter $c_s = \sqrt{\theta}$ is the sound speed in a gas close to equilibrium described by $M(\boldsymbol{v})$. Specifically, we assume

$$\langle 1, f^* \rangle = 1, \tag{7a}$$

$$\langle 1, \mathrm{V}_\alpha \mathrm{V}_\beta f^* \rangle = c_s^2 \delta_{\alpha\beta}, \tag{7b}$$

$$\langle 1, \mathrm{V}_\alpha \mathrm{V}_\beta \mathrm{V}_\gamma \mathrm{V}_\delta f^* \rangle = \kappa c_s^4 (\delta_{\alpha\beta}\delta_{\gamma\delta} + \delta_{\alpha\gamma}\delta_{\beta\delta} + \delta_{\alpha\delta}\delta_{\beta\gamma}), \tag{7c}$$

where $\kappa \neq d/(d+2)$ [see Eq. (10)]. The condition on κ excludes the D2Q6[1] model on a two-dimensional (2D) triangular lattice (without zero velocity) from our considerations for which it is known that the Navier-Stokes equation is obtained only after redefining the pressure. For the D2Q7 model on a 2D triangular lattice, the D2Q9 model on a 2D square lattice and the D3Q15 model on a three-dimensional (3D) cubic lattice, we find $\kappa = 1$ in accordance with the values of the Maxwellian fourth order moments. For the D2Q8 model on a 2D square lattice (without zero velocity), we find $\kappa = 5/9$. Based on f^*, we define the equilibrium distribution

$$f^{(\mathrm{eq})}(f) = F^{(\mathrm{eq})}(\langle 1, f \rangle, \langle 1, \mathbf{V}f \rangle),$$

which, for the sake of convenience, we split into a linear and a quadratic part:

$$f^{(\mathrm{eq})}(f) = f^{\mathrm{L(eq)}}(f) + f^{\mathrm{Q(eq)}}(f, f). \tag{8}$$

---

[1] We use notation DdQq for a q-velocity model in d dimensions.

The linear part is assumed of the form

$$f^{\mathrm{L(eq)}}(f) = F^{\mathrm{L(eq)}}(\langle 1, f \rangle, \langle 1, \mathbf{V}f \rangle), \qquad F^{\mathrm{L(eq)}}(\rho, \boldsymbol{u}) = (\rho + c_s^{-2}\boldsymbol{u} \cdot \mathbf{V})f^*$$

so that $f^* = F^{\mathrm{L(eq)}}(1, \mathbf{0})$ and, using (7a), (7b),

$$\left\langle 1, F^{\mathrm{L(eq)}}(\rho, \boldsymbol{u}) \right\rangle = \rho, \tag{9a}$$

$$\left\langle 1, \mathbf{V}F^{\mathrm{L(eq)}}(\rho, \boldsymbol{u}) \right\rangle = \boldsymbol{u}, \tag{9b}$$

$$\left\langle 1, \mathbf{V} \otimes \mathbf{V}F^{\mathrm{L(eq)}}(\rho, \boldsymbol{u}) \right\rangle = c_s^2 \rho \, \mathsf{I}. \tag{9c}$$

Here and in the following, I denotes the identity operator. To define the quadratic part, we first introduce the notations for the symmetric tensor product among two vectors $\boldsymbol{a}$ and $\boldsymbol{b}$:

$$(\boldsymbol{a} \otimes \boldsymbol{b})_{\alpha\beta} = \frac{1}{2}(a_\alpha b_\beta + a_\beta b_\alpha),$$

and the :-product between two matrices A and B

$$\mathsf{A} : \mathsf{B} = \sum_{\alpha,\beta=1}^{d} \mathsf{A}_{\alpha\beta}\mathsf{B}_{\alpha\beta}.$$

This allows us to write

$$f^{\mathrm{Q(eq)}}(f, g) = F^{\mathrm{Q(eq)}}(\langle 1, \mathbf{V}f \rangle, \langle 1, \mathbf{V}g \rangle), \qquad F^{\mathrm{Q(eq)}}(\boldsymbol{u}, \boldsymbol{w}) = (\boldsymbol{u} \otimes \boldsymbol{w}) : \Sigma f^*$$

where

$$\Sigma_{\alpha\beta} = \frac{1}{2\kappa c_s^4}\left[\mathrm{V}_\alpha \mathrm{V}_\beta - c_s^2 \delta_{\alpha\beta} + \frac{\kappa-1}{(d+2)\kappa-d}(|\mathbf{V}|^2 - dc_s^2)\delta_{\alpha\beta}\right]. \tag{10}$$

Note that the denominator $[(d+2)\kappa - d]$ leads to the constraint on the parameter $\kappa \neq d/(d+2)$. The structure of Σ combined with (7b), (7c) yields

$$\left\langle 1, F^{\mathrm{Q(eq)}}(\boldsymbol{u}, \boldsymbol{w}) \right\rangle = 0, \tag{11a}$$

$$\left\langle 1, \mathbf{V}F^{\mathrm{Q(eq)}}(\boldsymbol{u}, \boldsymbol{w}) \right\rangle = \mathbf{0}, \tag{11b}$$

$$\left\langle 1, \mathbf{V} \otimes \mathbf{V}F^{\mathrm{Q(eq)}}(\boldsymbol{u}, \boldsymbol{w}) \right\rangle = \boldsymbol{u} \otimes \boldsymbol{w}. \tag{11c}$$

Next, we list the conditions on the linear operator $\mathsf{A} : \mathcal{F} \to \mathcal{F}$.

(i) $\langle \mathsf{A}f, g \rangle = \langle f, \mathsf{A}g \rangle, \quad \forall \, f, g \in \mathcal{F}$;
(ii) A is positive semi-definite;
(iii) the even and odd functions form invariant subspaces of A
(iv) $\{1, v_1, \ldots, v_d\}$ generates the kernel of A;
(v) $\mathsf{A}(\Lambda f^*) = \frac{\kappa c_s^2}{\nu}\Lambda f^*$; where $\Lambda = \mathbf{V} \otimes \mathbf{V} - \frac{1}{d}|\mathbf{V}|^2\mathsf{I}$.

To give a specific example, we denote with Q the orthogonal projection onto the kernel of A and with $\mathsf{P} := \mathsf{I} - \mathsf{Q}$ the projection on the complement. Then $\mathsf{A} = \frac{1}{\tau}\mathsf{P}$

with $\tau = \nu/(\kappa c_s^2)$ is a particular choice which satisfies all conditions (i) to (v). Since $f^{(\mathrm{eq})}(f) - f$ is orthogonal to the kernel of A, which is easily checked by computing the scalar products with the elements of the kernel and observing (9) and (11), we have for any $\tau > 0$,

$$\frac{1}{\tau}\mathsf{P}[f^{(\mathrm{eq})}(f) - f] = \frac{1}{\tau}\left(\mathsf{Q} + \mathsf{P}\right)[f^{(\mathrm{eq})}(f) - f] = \frac{1}{\tau}[f^{(\mathrm{eq})}(f) - f].$$

Consequently, $\mathsf{A} = \frac{1}{\tau}\mathsf{P}$ is equivalent to the so called BGK collision operator $J(f) = \frac{1}{\tau}[f^{(\mathrm{eq})}(f) - f]$, which is the most popular LBE model [41, 6, 7, 47] and is only a special case considered here.

4. ASYMPTOTIC ANALYSIS OF FDVM WITH DIFFUSIVE SCALING

We shall demonstrate the use of the diffusive scaling to recover the incompressible Navier-Stokes equations as a limiting system. We begin with

$$\epsilon^2 \partial_t f_\epsilon + \epsilon \mathbf{V} \cdot \boldsymbol{\nabla} f_\epsilon = \mathsf{A}[f^{(\mathrm{eq})}(f_\epsilon) - f_\epsilon] \tag{12}$$

on a spatially periodic domain Ω. (Note that f_ϵ indicates the dependence of f on the perturbative parameter ϵ which is a continuous variable. It should not be confused with f_i in which the subscript i is an integer index for discrete velocities.) Because we only consider the incompressible regime, we specify the following initial values:

$$f_\epsilon|_{t=0} = F^{(\mathrm{eq})}(1, \epsilon \bar{\boldsymbol{u}}), \qquad \boldsymbol{\nabla} \cdot \bar{\boldsymbol{u}} = 0. \tag{13}$$

The above initial conditions guarantee that, initially, the density $\langle 1, f_\epsilon|_{t=0} \rangle = 1$ is a constant and that the velocity $\epsilon \bar{\boldsymbol{u}}(\boldsymbol{x}) = \langle 1, \mathbf{V} f_\epsilon|_{t=0} \rangle$ is small compared to the particle speed in the Boltzmann equation which is $\mathcal{O}(1)$ as $\epsilon \to 0$.

To investigate the asymptotic behavior of the initial value problem (12) with initial conditions (13) in the limit of $\epsilon \to 0$, we introduce a regular expansion

$$f_\epsilon = f^{(0)} + \epsilon f^{(1)} + \epsilon^2 f^{(2)} + \ldots$$

with $f^{(0)} = f^* = F^{(\mathrm{eq})}(1, \mathbf{0})$. Note that the initial values for the expansion coefficients $f^{(k)}$ are

$$f^{(1)}|_{t=0} = F^{\mathrm{L(eq)}}(0, \bar{\boldsymbol{u}}), \tag{14a}$$

$$f^{(2)}|_{t=0} = F^{\mathrm{Q(eq)}}(\bar{\boldsymbol{u}}, \bar{\boldsymbol{u}}), \tag{14b}$$

$$f^{(k)}|_{t=0} = 0, \qquad k \geq 3. \tag{14c}$$

Substituting the expansion of f_ϵ into (12) and setting $f^{(k)} = 0$ for $k < 0$, we obtain in order ϵ^{k+2}, $k \geq -2$, the following equation

$$\partial_t f^{(k)} + \mathbf{V} \cdot \boldsymbol{\nabla} f^{(k+1)} = \mathsf{A}\left[f^{\mathrm{L(eq)}}(f^{(k+2)}) - f^{(k+2)}\right.$$

$$\left. + \sum_{n+m=k+2} f^{\mathrm{Q(eq)}}(f^{(n)}, f^{(m)})\right]. \tag{15}$$

By induction, we can determine the expansion coefficients $f^{(1)}$, $f^{(2)}$, ... from the above relations. More precisely, Eq. (15) determines $f^{(k+2)}$ in terms of the lower order coefficients $f^{(l)}$, $l \leq k+1$ which have been obtained in previous steps. The procedure starts with $k = -1$, $f^{(-1)} = 0$ and $f^{(0)} = f^*$ to obtain $f^{(1)}$. The general procedure can be explained as follows.

We note that Eq. (15) is of the general form

$$\mathsf{A}z = b, \tag{16}$$

where the right hand side, b, contains the lower order coefficients:

$$b = \partial_t f^{(k)} + \mathbf{V} \cdot \boldsymbol{\nabla} f^{(k+1)} - \mathsf{A} \sum_{n+m=k+2} f^{\mathrm{Q(eq)}}(f^{(n)}, f^{(m)}), \tag{17}$$

and the unknown quantity z is the sum of terms involving $f^{(k+2)}$

$$z = f^{\mathrm{L(eq)}}(f^{(k+2)}) - f^{(k+2)}.$$

Since the vector space $\mathcal{F}$ is finite dimensional, Eq. (16) is a finite linear system and the solvability theory only involves basic linear algebra. Keeping in mind that A has a non-trivial kernel, we conclude that the image of A is *not* the whole space $\mathcal{F}$. In particular, Eq. (16) can only be solvable under certain restrictions on b. To formulate these restrictions, we note that if z solves Eq. (16) and if y is any element of the kernel, then

$$0 = \langle \mathsf{A}y, z \rangle = \langle y, \mathsf{A}z \rangle = \langle y, b \rangle$$

so that b has to be orthogonal to the kernel. In view of Eq. (17), the orthogonality conditions lead to a constraint on the moments $\rho^{(k)} = \langle 1, f^{(k)} \rangle$, $\boldsymbol{u}^{(k)} = \langle 1, \mathbf{V} f^{(k)} \rangle$, and $\mathsf{p}^{(k)} = \langle 1, \mathbf{V} \otimes \mathbf{V} f^{(k)} \rangle$:

$$\partial_t \rho^{(k)} + \boldsymbol{\nabla} \cdot \boldsymbol{u}^{(k+1)} = 0, \tag{18a}$$

$$\partial_t \boldsymbol{u}^{(k)} + \boldsymbol{\nabla} \cdot \mathsf{p}^{(k+1)} = \mathbf{0}. \tag{18b}$$

If these conditions are satisfied, and since b is in the orthogonal complement of the kernel which is equal to the image of A, we can uniquely determine the solution z of the system (16) which is orthogonal to the kernel. For notational convenience, we denote the inverse defined on the image of A by $\mathsf{A}^\dagger$, so that $z = \mathsf{A}^\dagger b$, or explicitly

$$f^{(k+2)} = f^{\mathrm{L(eq)}}(f^{(k+2)})$$
$$+ \sum_{n+m=k+2} f^{\mathrm{Q(eq)}}(f^{(n)}, f^{(m)}) - \mathsf{A}^\dagger \left[\partial_t f^{(k)} + \mathbf{V} \cdot \boldsymbol{\nabla} f^{(k+1)} \right]. \tag{19}$$

Note that (19) does not specify $f^{(k+2)}$ completely because $f^{(k+2)}$ also appears on the right hand side as argument of $f^{\mathrm{L(eq)}}$. Due to the structure of $f^{\mathrm{L(eq)}}$, the remaining degrees of freedom are $\rho^{(k+2)}$ and $\boldsymbol{u}^{(k+2)}$ which can be fixed using conditions (18a) and (18b).

In Appendix A.2 we exploit relations (18a), (18b) and (19) to determine the leading order coefficients of the expansion. For example,

$$f^{(1)} = c_s^{-2} \boldsymbol{u}^{(1)} \cdot \mathbf{V} f^*,$$
$$f^{(2)} = \rho^{(2)} f^* + F^{\mathrm{Q(eq)}}(\boldsymbol{u}^{(1)}, \boldsymbol{u}^{(1)}) - \frac{1}{2\kappa c_s^4} \nu (\boldsymbol{\nabla} \boldsymbol{u}^{(1)} + [\boldsymbol{\nabla} \boldsymbol{u}^{(1)}]^{\mathsf{T}}) : \Lambda f^*. \tag{20}$$

where $\boldsymbol{u}^{(1)}$ and $p^{(2)} = c_s^2 \rho^{(2)}$ satisfy the incompressible Navier-Stokes equations:

$$\boldsymbol{\nabla} \cdot \boldsymbol{u}^{(1)} = 0,$$
$$\partial_t \boldsymbol{u}^{(1)} + \boldsymbol{\nabla} \cdot (\boldsymbol{u}^{(1)} \otimes \boldsymbol{u}^{(1)}) + \boldsymbol{\nabla} p^{(2)} = \nu \boldsymbol{\nabla}^2 \boldsymbol{u}^{(1)}, \tag{21}$$
$$\boldsymbol{u}^{(1)}|_{t=0} = \bar{\boldsymbol{u}}.$$

with ν resulting from property (v) of the collision operator A. In contrast to the Chapman-Enskog expansion, the coefficients $f^{(1)}$ and $f^{(2)}$ are obviously given directly in terms of the solution to the target problem (21).

We remark that the structure of the distribution function $f^{(2)}$ is not compatible with the initial value (14b) unless $\bar{\boldsymbol{u}} = 0$. Similarly, incompatibilities with the initial values for the coefficients $f^{(k)}$ with $k \geq 3$ are observed if initial time derivatives of the Navier-Stokes solution do not vanish. This means that a regular expansion cannot accurately describe the initial evolution, or in other words, we expect an initial layer if the condition (13) is used (a phenomenon which is well known). This behavior can be carefully investigated using an initial layer expansion in the time scale t/ϵ. It is also possible to avoid the initial layer by modifying the initialization (13) in such a way that it is compatible with the expansion. A detailed discussion of this phenomenon is deferred elsewhere [4].

For the higher order coefficients $f^{(3)}$, $f^{(4)}$, ... we show in Appendix A.2 that $f^{(k)}/f^*$ is an even (odd) polynomial with respect to the velocity variable provided k is even (odd). As a consequence, $\boldsymbol{u}^{(2n)} = 0$ and $\rho^{(2n+1)} = 0$ for all n so that the density and velocity moments of the solution f_ϵ of (12) have the following forms:

$$\boldsymbol{u}_\epsilon = \epsilon \boldsymbol{u}^{(1)} + \epsilon^3 \boldsymbol{u}^{(3)} + \epsilon^5 \boldsymbol{u}^{(5)} + \dots$$
$$\rho_\epsilon = 1 + \epsilon^2 \rho^{(2)} + \epsilon^4 \rho^{(4)} + \epsilon^6 \rho^{(6)} + \dots. \tag{22}$$

The higher order moments $\boldsymbol{u}^{(k+1)}$ and $p^{(k+2)} = c_s^2 \rho^{(k+2)}$ with indices $k = 2n$, $n \geq 1$ are the solutions of *linear* Oseen-type equations

$$\boldsymbol{\nabla} \cdot \boldsymbol{u}^{(k+1)} = -\partial_t \rho^{(k)},$$
$$\partial_t \boldsymbol{u}^{(k+1)} + 2 \boldsymbol{\nabla} \cdot (\boldsymbol{u}^{(1)} \otimes \boldsymbol{u}^{(k+1)}) + \boldsymbol{\nabla} p^{(k+2)} = \nu \boldsymbol{\nabla}^2 \boldsymbol{u}^{(k+1)} + \boldsymbol{B}^{(k)},$$
$$\boldsymbol{u}^{(k+1)}|_{t=0} = 0, \quad \rho^{(k+2)}|_{t=0} = 0,$$

where the source term $\boldsymbol{B}^{(k)}$ is obtained from lower order moments. We note that Eq. (22) can be rewritten as:

$$\frac{1}{\epsilon} \boldsymbol{u}_\epsilon - \boldsymbol{u}^{(1)} = \epsilon^2 \boldsymbol{u}^{(3)} + \dots,$$
$$\frac{1}{\epsilon^2} c_s^2 (\rho_\epsilon - 1) - p^{(2)} = \epsilon^2 c_s^2 \rho^{(4)} + \dots.$$

This observation can be used as a rigorous argument to show that the rescaled lattice Boltzmann moments $\boldsymbol{u}_\epsilon/\epsilon$ and $c_s^2(\rho_\epsilon - 1)/\epsilon^2$ converge to the solutions $\boldsymbol{u}^{(1)}$ and $p^{(2)}$ of the incompressible Navier-Stokes equations [27].

5.   ASYMPTOTIC ANALYSIS OF THE LBE

Before we proceed to the analysis of the lattice Boltzmann equation, let us briefly outline the general framework which is applicable to any finite difference scheme for differential equations. To formulate the prerequisites of the analysis let us assume that the finite difference equations are implemented in the form of a computer program. The program should depend on a parameter ϵ (grid spacing) which determines the total number $N(\epsilon)$ of equations for the unknown values $\hat{w}_1$, ..., $\hat{w}_{N(\epsilon)}$. The parameter $N(\epsilon)$ may explicitly appear in the equations. To incorporate data like boundary conditions or source terms and to display the results, the program includes a certain scaling which relates unknowns $\hat{w}_i$ and data values $\hat{d}_i$ to points $y_i(\epsilon)$ in the interested domain. In particular, for decreasing ϵ, the points $y_i(\epsilon)$ and the discrete solution consisting of all pairs $(y_i(\epsilon), \hat{w}_i)$ become increasingly dense. If this numerical solution appears to be smooth, then it is then natural to assume that $\hat{w}_i$ can be described by a smooth function, for example, in the form of a regular expansion

$$\hat{w}_i = w^{(0)}(y_i(\epsilon)) + \epsilon w^{(1)}(y_i(\epsilon)) + \epsilon^2 w^{(2)}(y_i(\epsilon)) + \dots \qquad (23)$$

with smooth functions $\{w^{(k)}\}$. This brief introduction already summarizes all the requirements (the difference equations and the scaling) as well as a first approach on how to analyze the result, namely by a regular expansion. Note that *no* knowledge of the origin of the discrete equations is required. If we substitute the expansion (23) into the difference equations, which define the algorithm, and Taylor-expand the difference equations, we can derive differential equations for the expansion coefficients $\{w^{(k)}\}$. If this is accomplished, one can conclude that, in the leading order, the discrete values $\hat{w}_i$ approximate point values of the solution $w^{(0)}$ to the leading order differential equation. The accuracy of the approximation can be obtained by investigating the equations for the higher order coefficients $w^{(1)}$, $w^{(2)}$, ... If the equation satisfied by $w^{(1)}$ has non-trivial general solutions, the approximation is only first order accurate, but if $w^{(1)}$ can be shown to be zero, then the approximation is at least of second order in ϵ. In general if the leading n terms $\{w^{(k)}, \ k = 1, 2, \dots, n\}$ vanish, then then approximation is at least of $(n + 1)$-th order. Since the first non-zero higher order coefficient is the leading order error contribution, an analysis of the equation for this coefficient provides an indication of the size of the error and its dependence on the solution $w^{(0)}$.

If the result of the finite difference scheme shows irregular behavior like interior or boundary layers (*e.g.*, [8]), grid oscillations or other phenomena which vary significantly on the grid scale, then the assumption of a regular expansion is inadequate and will result in a contradiction with the assumed smoothness of one of the coefficients, thus *predicting* phenomena on the grid scale up to a certain order. In this case, one can either use *irregular* expansions to analyze the non-smooth phenomenon in detail (*e.g.*, [26]), or identify the inconsistencies and then modify the scheme to remove them.

After this introductory overture, we now apply this approach to our particular case, the lattice Boltzmann equation. The data of the problem are given by a smooth, divergence free initial velocity field $\bar{\boldsymbol{u}} : \mathbb{R}^d \to \mathbb{R}^d$ which is periodic, and a source term $g : \mathbb{R}_0^+ \times \mathbb{R}^d \times \mathbb{V} \to \mathbb{R}$ which is also smooth, periodic in space $\boldsymbol{x}$, and with odd symmetry in the third argument. The odd symmetry assures that g leads to a momentum flux but not to an immediate mass flux. The unknowns in the lattice Boltzmann equation are labeled by $(n, \boldsymbol{j}, \boldsymbol{v}) \in \mathbb{N}_0 \times \mathbb{X} \times \mathbb{V}$ where n indicates the time step, $\boldsymbol{j} \in \mathbb{X} \subset \mathbb{R}^d$ a lattice point and $\boldsymbol{v} \in \mathbb{V}$ a discrete velocity. Using these notations, we introduce the following scaling

$$(n, \boldsymbol{j}, \boldsymbol{v}) \to (t_n(\epsilon), \boldsymbol{x_j}(\epsilon), \boldsymbol{v}) = (\epsilon^2 n, \epsilon \boldsymbol{j}, \boldsymbol{v}) \in \mathbb{R}_0^+ \times \mathbb{R}^d \times \mathbb{V}, \qquad \epsilon > 0$$

which associates time-space-velocity points to the grid labels. Note that this scaling incorporates the relation $\Delta t = \epsilon^2 = \Delta x^2$ between space and time increments which reflects the diffusive scaling and leads to a physically interesting limiting behavior in the case of the finite discrete-velocity model, as discussed in Sec. 4.

The lattice Boltzmann equation we consider, has the form

$$\hat{f}(n+1, \boldsymbol{j} + \boldsymbol{v}, \boldsymbol{v}) - \hat{f}(n, \boldsymbol{j}, \boldsymbol{v}) = \mathsf{A}[f^{(\text{eq})}(\hat{f}) - \hat{f}](n, \boldsymbol{j}, \boldsymbol{v}) \\ + \lambda \hat{g}(n, \boldsymbol{j}, \boldsymbol{v}) + (1 - \lambda) \hat{g}(n+1, \boldsymbol{j} + \boldsymbol{v}, \boldsymbol{v}) \quad (24)$$

with the initialization

$$\hat{f}(0, \boldsymbol{j}, \cdot) = F^{(\text{eq})}\left(1, \epsilon \bar{\boldsymbol{u}}(\boldsymbol{x_j}(\epsilon))\right) \tag{25}$$

and the discrete source term

$$\hat{g}(n, \boldsymbol{j}, \boldsymbol{v}) = \epsilon^3 g(t_n(\epsilon), \boldsymbol{x_j}(\epsilon), \boldsymbol{v}). \tag{26}$$

The parameter λ in (24) should satisfy $0 \leq \lambda \leq 1$. We remark that the low Mach number assumption is built into (25) because we initialize with a velocity $\epsilon \bar{\boldsymbol{u}}$ of order ϵ and because we make sure that the increase of velocity during each time step is of the order $\epsilon \Delta t = \epsilon^3$ by scaling the force term g with an appropriate factor.

Similar to our considerations in Sec. 4, we assume a regular expansion of the following form

$$\hat{f}(n, \boldsymbol{j}, \boldsymbol{v}) = f^*(\boldsymbol{v}) + \epsilon f^{(1)}(t_n(\epsilon), \boldsymbol{x_j}(\epsilon), \boldsymbol{v}) + \epsilon^2 f^{(2)}(t_n(\epsilon), \boldsymbol{x_j}(\epsilon), \boldsymbol{v}) + \dots \tag{27}$$

with smooth coefficient functions $f^{(m)}$ which are periodic in the second argument. Note that the moments

$$\rho^{(m)} = \left\langle 1, f^{(m)} \right\rangle, \qquad \boldsymbol{u}^{(m)} = \left\langle 1, \mathbf{V} f^{(m)} \right\rangle, \qquad \mathsf{p}^{(m)} = \left\langle 1, \mathbf{V} \otimes \mathbf{V} f^{(m)} \right\rangle$$

inherit the periodicity and smoothness from the coefficients $f^{(m)}$.

From hereafter, the analysis is straightforward: the expansion is inserted into Eq. (24) and Taylor expansion is employed to transform difference expressions into differential operators.

We start by substituting Eq. (27) into the left hand side of (24). This leads to expressions of the following form:

$$f^{(m)}(t_n + \epsilon^2, \boldsymbol{x_j} + \epsilon\boldsymbol{v}, \boldsymbol{v}) - f^{(m)}(t_n, \boldsymbol{x_j}, \boldsymbol{v}) = \epsilon(\boldsymbol{v}\cdot\boldsymbol{\nabla})f^{(m)}$$
$$+ \epsilon^2(\partial_t + (\boldsymbol{v}\cdot\boldsymbol{\nabla})^2/2)f^{(m)} + \epsilon^3(\boldsymbol{v}\cdot\boldsymbol{\nabla})(\partial_t + (\boldsymbol{v}\cdot\boldsymbol{\nabla})^2/6)f^{(m)} + \dots$$

where the right hand side is evaluated at $(t_n, \boldsymbol{x_j}, \boldsymbol{v})$ and the argument ϵ of t_n and $\boldsymbol{x_j}$ is suppressed for brevity. Generalizing this expansion to arbitrary orders, we formally obtain an infinite series:

$$f^{(m)}(t_n + \epsilon^2, \boldsymbol{x_j} + \epsilon\boldsymbol{v}, \boldsymbol{v}) - f^{(m)}(t_n, \boldsymbol{x_j}, \boldsymbol{v}) = \sum_{r=0}^{\infty} \epsilon^r D_r(\partial_t, \boldsymbol{v}\cdot\boldsymbol{\nabla})f^{(m)}(t_n, \boldsymbol{x_j}, \boldsymbol{v}),$$

where $D_r(\tau, \sigma)$ are polynomials, specifically,

$$D_0(\tau, \sigma) = 0, \quad D_1(\tau, \sigma) = \sigma, \quad D_2(\tau, \sigma) = \tau + \sigma^2/2, \quad D_3(\tau, \sigma) = \sigma(\tau + \sigma^2/6),$$

or more generally

$$D_r(\tau, \sigma) = \sum_{2a+b=r} \frac{\tau^a \sigma^b}{a!b!}, \qquad r \geq 1.$$

The important observation is that, if r is even, $D_r(\tau, \sigma)$ is an even polynomial in σ because $(2a + b)$ can be even only if b is even. Conversely, $D_r(\tau, \sigma)$ is odd in σ if r is odd.

With definition (26), an expansion of the source term on the right hand side of Eq. (24) yields similarly

$$\lambda\hat{g}(n, \boldsymbol{j}, \boldsymbol{v}) + (1 - \lambda)\hat{g}(n + 1, \boldsymbol{j} + \boldsymbol{v}, \boldsymbol{v}) = \sum_{m=0}^{\infty} \epsilon^m g^{(m)}(t_n, \boldsymbol{x_j}, \boldsymbol{v})$$

with

$$g^{(0)} = g^{(1)} = g^{(2)} = 0, \quad g^{(3)} = g, \quad g^{(3+r)} = (1 - \lambda)D_r(\partial_t, \mathbf{V}\cdot\boldsymbol{\nabla})g, \quad r \geq 1.$$

Note that, as a function of $\boldsymbol{v}$, $g^{(m)}$ is odd (even) if m is odd (even) because g is assumed to be odd and $D_r(\partial_t, \mathbf{V}\cdot\boldsymbol{\nabla})$ is an odd (even) polynomial in $\mathbf{V}$ for an odd (even) r.

Since the collision operator acts locally in time and space, no further Taylor expansion is required and only a shuffling of orders appears because of the quadratic nonlinearity. Consequently, we obtain in order ϵ^{k+2} for $k \geq -2$ (cf. Sec. 4 for the choice of k):

$$\sum_{m+r=k+2} D_r(\partial_t, \mathbf{V}\cdot\boldsymbol{\nabla})f^{(m)} - g^{(k+2)}$$
$$= \mathsf{A}\left[f^{\mathrm{L(eq)}}(f^{(k+2)}) - f^{(k+2)} + \sum_{m+r=k+2} f^{\mathrm{Q(eq)}}(f^{(r)}, f^{(m)})\right]. \quad (28)$$

We have omitted some technical details in deriving (28), *i.e.*, the fact that all Taylor expansions above are carried out around the discrete points $(t_n(\epsilon), \boldsymbol{x_j}(\epsilon), \boldsymbol{v})$ which are ϵ-dependent. In order to obtain the leading order equation (28) at an *arbitrary* point $(t, \boldsymbol{x}, \boldsymbol{v})$, we have to choose a grid sequence based on $(\epsilon_m)_{m\in\mathbb{N}}$ with $\epsilon_m \to 0$ and a sequence of labels $(n_m, \boldsymbol{j}_m, \boldsymbol{v})$ such that

$$(t_{n_m}(\epsilon_m), \boldsymbol{x_{j_m}}(\epsilon_m), \boldsymbol{v}) \xrightarrow[m\to\infty]{} (t, \boldsymbol{x}, \boldsymbol{v}).$$

Once the leading order condition is obtained, it can be removed from the expansion and after division by ϵ, the next condition (28) can be constructed in the same way. For further details, we refer to [26].

To work out the similarities of (28) to the expression (15), we note that

$$\sum_{m+r=k+2} D_r(\partial_t, \mathbf{V} \cdot \boldsymbol{\nabla}) f^{(m)} = (\mathbf{V} \cdot \boldsymbol{\nabla}) f^{(k+1)} + \partial_t f^{(k)} + \frac{1}{2}(\mathbf{V} \cdot \boldsymbol{\nabla})^2 f^{(k)} + \dots$$

Introducing the term

$$L^{(k+2)} = g^{(k+2)} - \sum_{\substack{m+r=k+2 \\ m<k}} D_r(\partial_t, \mathbf{V} \cdot \boldsymbol{\nabla}) f^{(m)} \tag{29}$$

we thus have

$$\sum_{m+r=k+2} D_r(\partial_t, \mathbf{V} \cdot \boldsymbol{\nabla}) f^{(m)} - g^{(k+2)} = \partial_t f^{(k)} + (\mathbf{V} \cdot \boldsymbol{\nabla}) f^{(k+1)}$$
$$+ \frac{1}{2}(\mathbf{V} \cdot \boldsymbol{\nabla})^2 f^{(k)} - L^{(k+2)}.$$

so that the left hand side of (28) differs from the one of (15) only in the terms $(\mathbf{V} \cdot \boldsymbol{\nabla})^2 f^{(k)}/2$ and $L^{(k+2)}$. In particular, we can use the same analysis as for the FDVM case and mainly have to track the influence of the additional terms. For example, the solvability conditions (18a) and (18b) are now of the form

$$\partial_t \rho^{(k)} + \boldsymbol{\nabla} \cdot \boldsymbol{u}^{(k+1)} + \frac{1}{2}\boldsymbol{\nabla} \otimes \boldsymbol{\nabla} : \mathsf{p}^{(k)} = \left\langle 1, L^{(k+2)} \right\rangle, \tag{30a}$$

$$\partial_t \boldsymbol{u}^{(k)} + \boldsymbol{\nabla} \cdot \mathsf{p}^{(k+1)} + \frac{1}{2}\left\langle 1, \mathbf{V}(\mathbf{V} \cdot \boldsymbol{\nabla})^2 f^{(k)} \right\rangle = \left\langle 1, \mathbf{V} L^{(k+2)} \right\rangle, \tag{30b}$$

and $\mathsf{A}^\dagger$ applied to (28) yields the analog of (19)

$$f^{(k+2)} = f^{\mathrm{L(eq)}}(f^{(k+2)}) + \sum_{m+r=k+2} f^{\mathrm{Q(eq)}}(f^{(r)}, f^{(m)})$$
$$- \mathsf{A}^\dagger \left[\partial_t f^{(k)} + \mathbf{V} \cdot \boldsymbol{\nabla} f^{(k+1)} + \frac{1}{2}(\mathbf{V} \cdot \boldsymbol{\nabla})^2 f^{(k)} \right] + \mathsf{A}^\dagger L^{(k+2)}. \tag{31}$$

The details of the analysis are given in Appendix A.3. For the expansion coefficients $f^{(1)}$ and $f^{(2)}$ we find the same structure (20) as in the case of the FDVM. However, the moments $\boldsymbol{u}^{(1)}$ and $p^{(2)} = c_s^2 \rho^{(2)}$ now satisfy the incompressible Navier-Stokes

equation with an additional force field $\boldsymbol{G} = \langle 1, \mathbf{V}g \rangle$ and the well known viscosity modification

$$\boldsymbol{\nabla} \cdot \boldsymbol{u}^{(1)} = 0,$$

$$\partial_t \boldsymbol{u}^{(1)} + \boldsymbol{\nabla} \cdot (\boldsymbol{u}^{(1)} \otimes \boldsymbol{u}^{(1)}) + \boldsymbol{\nabla} p^{(2)} = (\nu - \frac{1}{2}\kappa c_s^2)\boldsymbol{\nabla}^2 \boldsymbol{u}^{(1)} + \boldsymbol{G},$$

$$\boldsymbol{u}^{(1)}|_{t=0} = \bar{\boldsymbol{u}}.$$

So far, the analysis shows that the discrete density and velocity values

$$\hat{\rho}(n, \boldsymbol{j}) = \left\langle 1, \hat{f}(n, \boldsymbol{j}, \cdot) \right\rangle, \qquad \hat{\boldsymbol{u}}(n, \boldsymbol{j}) = \left\langle 1, \mathbf{V}\hat{f}(n, \boldsymbol{j}, \cdot) \right\rangle$$

are, in leading order, given by a solution of the Navier-Stokes equation

$$\hat{\rho}(n, \boldsymbol{j}) = 1 + \epsilon^2 c_s^{-2} p^{(2)}(t_n(\epsilon), \boldsymbol{x}_{\boldsymbol{j}}(\epsilon)) + \ldots,$$

$$\hat{\boldsymbol{u}}(n, \boldsymbol{j}) = \epsilon \boldsymbol{u}^{(1)}(t_n(\epsilon), \boldsymbol{x}_{\boldsymbol{j}}(\epsilon)) + \ldots.$$

The order of accuracy follows from the investigation of higher order terms. As in the case of the FDVM, the coefficients $f^{(m)}$ are odd (even) if the index m is odd (even) so that the moments $\boldsymbol{u}^{(2n)}$ and $\rho^{(2n+1)}$ vanish for all n. The remaining fields $\boldsymbol{u}^{(k+1)}$ and $\rho^{(k+2)}$ with even $k \geq 2$ are solutions to Oseen-type problems (in analogy to the FDVM case)

$$\boldsymbol{\nabla} \cdot \boldsymbol{u}^{(k+1)} = \left\langle 1, L^{(k+2)} \right\rangle - \partial_t \rho^{(k)} - \frac{1}{2}\boldsymbol{\nabla} \otimes \boldsymbol{\nabla} : \mathsf{p}^{(k)},$$

$$\partial_t \boldsymbol{u}^{(k+1)} + 2\boldsymbol{\nabla} \cdot (\boldsymbol{u}^{(1)} \otimes \boldsymbol{u}^{(k+1)}) + \boldsymbol{\nabla} p^{(k+2)} = \left(\nu - \frac{1}{2}\kappa c_s^2\right) \boldsymbol{\nabla}^2 \boldsymbol{u}^{(k+1)} + \boldsymbol{C}^{(k)},$$

$$\boldsymbol{u}^{(k+1)}|_{t=0} = 0, \quad \rho^{(k+2)}|_{t=0} = 0,$$

where $\boldsymbol{C}^{(k)}$ depends on lower order coefficients and is, in general, non-zero. Hence $\rho^{(4)}$ and $\boldsymbol{u}^{(3)}$ will typically not vanish. In terms of consistency, this result implies that the numerical values $\hat{\rho}(n, \boldsymbol{j})$ and $\hat{\boldsymbol{u}}(n, \boldsymbol{j})$ yield at least second order accurate approximations of the Navier-Stokes solution because

$$\frac{1}{\epsilon^2} c_s^2 (\hat{\rho} - 1) - p^{(2)} = \epsilon^2 c_s^2 p^{(4)} + \ldots,$$

$$\frac{1}{\epsilon} \hat{\boldsymbol{u}} - \boldsymbol{u}^{(1)} = \epsilon^2 \boldsymbol{u}^{(3)} + \ldots.$$

In these relations, the discrete quantities are evaluated at $(n, \boldsymbol{j})$ and the continuous coefficients at the corresponding nodes $(t_n(\epsilon), \boldsymbol{x}_{\boldsymbol{j}}(\epsilon))$. Note that, in view of the scaling rule $\Delta t = \Delta x^2 = \epsilon^2$, second order accuracy with respect to ϵ means only *first* order accuracy in time because the time step is ϵ^2. However, the accuracy in space is second order.

We conclude with a comment on the choice of g. If a prescribed field $\boldsymbol{G}(t, \boldsymbol{x})$ should appear as force term in the Navier-Stokes equation, one can choose

$$g(t, \boldsymbol{x}, \boldsymbol{v}) = c_s^{-2} \boldsymbol{v} \cdot \boldsymbol{G}(t, \boldsymbol{x}) f^*(\boldsymbol{v}) \tag{32}$$

because in this case

$$\langle 1, \mathbf{V}g\rangle = c_s^{-2} \langle 1, \mathbf{V} \otimes \mathbf{V}f^*\rangle \, \boldsymbol{G} = \boldsymbol{G}.$$

We also note that the convex combination parameter λ in Eq. (24) plays no role in leading order. Its effects on the error will be discussed in the following section. An expression somewhat different from Eq. (32) has been introduced in [30, 31, 34] where a forcing term is derived based on a Grad-expansion

$$\hat{g}(n, \boldsymbol{j}, \boldsymbol{v}) = \frac{\epsilon^3}{c_s^2}\bigg(\boldsymbol{G}(t_n, \boldsymbol{x}_j) \cdot (\boldsymbol{v} - \hat{\boldsymbol{u}}(n, \boldsymbol{j})) + (\boldsymbol{G}(t_n, \boldsymbol{x}_j) \cdot \boldsymbol{v})(\hat{\boldsymbol{u}}(n, \boldsymbol{j}) \cdot \boldsymbol{v})) \bigg) f^*(\boldsymbol{v}).$$

Note that this function does not have the odd symmetry required in our analysis. However, since $\hat{\boldsymbol{u}}$ is only of order ϵ, the even contributions start in order ϵ^4

$$\hat{g} = \frac{\epsilon^3}{c_s^2}\boldsymbol{G} \cdot \mathbf{V}f^* + \frac{\epsilon^4}{c_s^2}(\boldsymbol{G} \cdot \boldsymbol{u}^{(1)} + (\boldsymbol{G} \cdot \mathbf{V})(\boldsymbol{u}^{(1)} \cdot \mathbf{V}))f^* + \mathcal{O}(\epsilon^5)$$

which is just sufficient to show that $\boldsymbol{u}^{(1)}$ and $\rho^{(2)}$ are given by a Navier-Stokes solution and that $\boldsymbol{u}^{(2)} = 0$ and $\rho^{(3)} = 0$. Hence, this force term also leads to a second order scheme.

6.   2D TAYLOR-VORTEX FLOW: A TEST CASE

As we have shown in the previous section, the asymptotic analysis can be used to verify consistency of a finite difference scheme and to predict the consistency order. In this section, we would like to show that it also yields correct information about the leading order error term. Such information is valuable if one intends to improve the order of the method by removing the leading order error. The need for improvements is obvious in flow problems on non-periodic domains where boundary conditions like the bounce-back conditions typically reduce the consistency of the pressure to first or even zero order in lattice BGK scheme (cf. [25]). In contrast, the situation on periodic domains is rather academical. Nevertheless, the example is useful to show that the leading order error is *correctly* predicted by the asymptotic analysis and this is our main motivation here.

We only remark in passing that a higher order method for the periodic problem can be obtained using the classical method of Richardson extrapolation. If the numerical solution $\hat{\boldsymbol{u}}(n, \boldsymbol{j})/\epsilon$, $\hat{p}(n, \boldsymbol{j}) = c_s^2(\hat{\rho}(n, \boldsymbol{j}) - 1)/\epsilon^2$ can be expressed in terms of regular expansions with ϵ-independent coefficients

$$\hat{p}(n, \boldsymbol{j}) = p^{(2)}(t_n, \boldsymbol{x}_j) + \epsilon^2 p^{(4)}(t_n, \boldsymbol{x}_j) + \epsilon^4 p^{(6)}(t_n, \boldsymbol{x}_j) + \dots,$$
$$\frac{1}{\epsilon}\hat{\boldsymbol{u}}(n, \boldsymbol{j}) = \boldsymbol{u}^{(1)}(t_n, \boldsymbol{x}_j) + \epsilon^2 \boldsymbol{u}^{(3)}(t_n, \boldsymbol{x}_j) + \epsilon^4 \boldsymbol{u}^{(5)}(t_n, \boldsymbol{x}_j) + \dots,$$

then $\boldsymbol{u}^{(3)}$ and $p^{(4)}$ can be removed by combining the solutions obtained on two different grids. Taking, for example, the solution based on grid-size ϵ with weight -1 and the solution for the finer grid $\epsilon/2$ with factor 4, the leading error terms drops out upon addition and subsequent division of the result by 3 yields the Navier-Stokes solution up to fourth order. To numerically support this consideration, we consider

the 2D Taylor-vortex flow in a periodic domain as a test case:

$$\bar{u}_1(t, \boldsymbol{x}) = -\frac{1}{a}\cos(ax_1)\sin(bx_2)\exp(-\tilde{\nu}(a^2 + b^2)t),$$

$$\bar{u}_2(t, \boldsymbol{x}) = \frac{1}{b}\sin(ax_1)\cos(bx_2)\exp(-\tilde{\nu}(a^2 + b^2)t),$$

$$\bar{p}(t, \boldsymbol{x}) = -\frac{1}{4}\left[a^{-2}\cos(2ax_1) + b^{-2}\cos(2bx_2)\right]\exp(-2\tilde{\nu}(a^2 + b^2)t),$$

which $a = b = 2\pi$. To avoid initial layers which introduce a temporal oscillation on a faster time scale and lead to ϵ-dependent expansion coefficients (thus contradicting the assumption underlying the Richardson procedure), we use a modification

$$\boldsymbol{u}(t, \boldsymbol{x}) = \alpha(t)\bar{\boldsymbol{u}}(t, \boldsymbol{x}), \qquad p(t, \boldsymbol{x}) = \alpha(t)\bar{p}(t, \boldsymbol{x})$$

with a smooth function α satisfying $\alpha(0) = 0$ (to guarantee that initial layers are suppressed in the ϵ orders considered here, we choose $\alpha(t) = t^3$). It is easy to check that these fields satisfy the Navier-Stokes equation with zero initial values, if we introduce the force term

$$\boldsymbol{G} = \alpha'\bar{\boldsymbol{u}} + (\alpha - 1)\alpha\boldsymbol{\nabla}\cdot(\bar{\boldsymbol{u}}\otimes\bar{\boldsymbol{u}}).$$

The force term $\boldsymbol{G}$ is incorporated into the lattice Boltzmann evolution using the form (32) and $\lambda = 1$. As collision operator we take the BGK approximation with relaxation parameter $\tau = \nu/(\kappa c_s^2)$. The corresponding lattice Boltzmann scheme approximates solutions to the Navier-Stokes equation (A.16) with effective viscosity $\tilde{\nu} = \nu - \kappa c_s^2/2$ which we use in the definition of the functions $\bar{\boldsymbol{u}}$ and $\bar{p}$. In what follows, we set $\tilde{\nu} = 0.01$.

Calculating the solution on 10×10, 20×20, 40×40 and 80×80 grids and plotting the numerical error in pressure and velocity in a log-log plot *versus* the grid size ϵ at $t = 0.5$, the increase of the order manifests itself in an increased slope of the Richardson solution, as shown in Fig. 1. Note that the Richardson procedure requires two grids for a single solution so that only the errors for 20×20, 40×40, and 80×80 grids are presented. A second remark concerns the normalization of the pressure. Since the pressure in the Navier-Stokes equation is only unique up to constants, we generally face the problem that the pressure of an exact solution may have a different normalization than the numerical pressure. In our example above, this could lead to a second order behavior of the pressure error in connection with the Richardson procedure simply because the difference of the two arbitrary pressure constants remains at second order. To remove this arbitrary constant, we subtract the arithmetic grid average from the final pressure approximation instead of the constant value one and compare with the exact pressure where the grid average is also subtracted.

Another consequence which follows simply from the existence of the regular expansion is the accuracy of finite difference derivative approximations of the solution. Consider, for example, the approximation of the vorticity $\omega^{(1)} = \partial_1 u_2^{(1)} - \partial_2 u_1^{(1)}$ which is not available directly as a velocity moment of the kinetic variables. If we approximate $\omega^{(1)}$ by central differences (division by ϵ^2 is needed because $\hat{\boldsymbol{u}}/\epsilon$
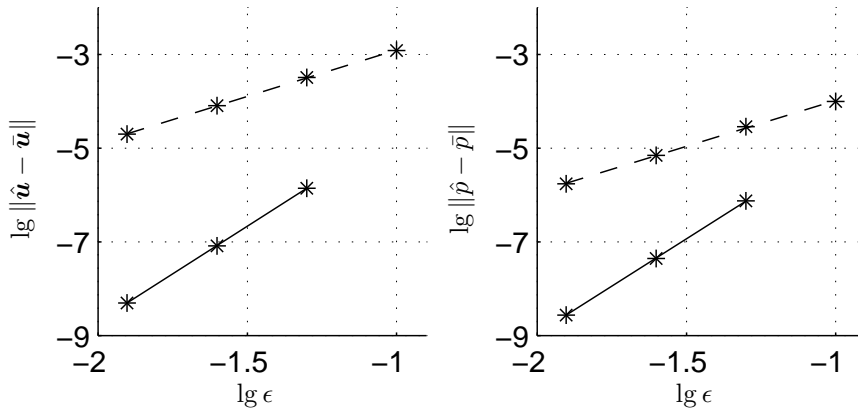
FIG. 1. Error behavior of velocity (left) and pressure (right) using the LBE (dashed) and the LBE with Richardson extrapolation (solid). The least-square slopes are 1.98 and 4.07 for the velocity and 1.96 and 4.04 for the pressure, respectively.

approximates $\boldsymbol{u}^{(1)}$):

$$\hat{\omega}(n, \boldsymbol{j}) = \frac{1}{2\epsilon^2} \left[\hat{u}_2(n, \boldsymbol{j} + \boldsymbol{e}_1) - \hat{u}_2(n, \boldsymbol{j} - \boldsymbol{e}_1) \right] - \frac{1}{2\epsilon^2} \left[\hat{u}_1(n, \boldsymbol{j} + \boldsymbol{e}_2) - \hat{u}_1(n, \boldsymbol{j} - \boldsymbol{e}_2) \right],$$

the question concerning the accuracy of $\hat{\omega}$ arises. Inserting the expansion for $\hat{\boldsymbol{u}}$ into the expression for $\hat{\omega}$ and performing a Taylor expansion, we find, up to terms of order ϵ^4,

$$\hat{\omega} = \omega^{(1)} + \frac{\epsilon^2}{6} \left(\partial_1^3 u_2^{(1)} - \partial_2^3 u_1^{(1)} \right) + \epsilon^2 \omega^{(3)} + \mathcal{O}(\epsilon^4)$$

where $\omega^{(3)}$ is the vorticity corresponding to the velocity field $\boldsymbol{u}^{(3)}$. We see that $\hat{\omega} - \omega^{(1)} = \mathcal{O}(\epsilon^2)$, *i.e.*, the finite difference approximation is second order accurate. The above argument breaks down if the field $\boldsymbol{u}^{(3)}$ is not ϵ-independent (*e.g.*, if $\boldsymbol{u}^{(3)}$ varies in order one between two grid points). Then the discrete derivative may be of order $1/\epsilon$ which would reduce the accuracy to order one. However, in the periodic case considered here, this is not the case and thus we observe second order accuracy. For the test problem above, the numerical vorticity $\hat{\omega}$ is compared with the exact one $\omega^{(1)}$ at $t = 0.5$ (using $\lambda = 1$) in Fig. 2.

While the Richardson procedure and the statement about the accuracy of finite difference derivative approximations requires only the existence of a regular expansion, we would also like to show that the structure of the coefficients is correctly given in the expansion. To demonstrate this, we concentrate on the role of the parameter λ in our LB scheme. As we have seen in the previous section, λ does not affect the behavior of the scheme in the leading order. However, two numerical solutions calculated with two different values λ_1 and λ_2 will not exhibit the same numerical error. To predict the difference $\delta\hat{\boldsymbol{u}}$ of the velocity fields and $\delta\hat{\rho}$ of the densities, we consider the equation for the leading order errors $\boldsymbol{u}^{(3)}$ and $\rho^{(4)}$ in Appendix A.4. It turns out that the difference of the leading error terms is given by

$$\delta\boldsymbol{u}^{(3)} = \boldsymbol{w} - \delta\lambda \boldsymbol{G}, \qquad \delta\rho^{(4)} = q/c_s^2$$
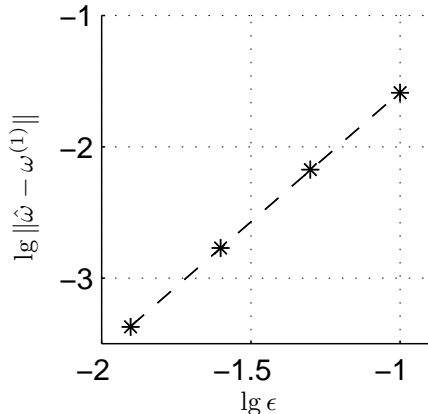
FIG. 2.   The vorticity error *versus* ϵ. The least-square slope is 1.98.

where $\delta\lambda = \lambda_1 - \lambda_2$ and $\boldsymbol{w}$ and q solve

$$\boldsymbol{\nabla}\cdot\boldsymbol{w} = 0,$$

$$\partial_t\boldsymbol{w} + 2\boldsymbol{\nabla}\cdot(\boldsymbol{u}^{(1)}\otimes\boldsymbol{w}) + \boldsymbol{\nabla}q = \left(\nu - \frac{1}{2}\kappa c_s^2\right)\boldsymbol{\nabla}^2\boldsymbol{w} + 2\delta\lambda\boldsymbol{\nabla}\cdot(\boldsymbol{u}^{(1)}\otimes\boldsymbol{G}),$$

$$\boldsymbol{w}|_{t=0} = 0, \quad q|_{t=0} = \boldsymbol{0},$$

To verify whether this prediction can be numerically recovered, we perform the following test: we run the LB scheme (24) for the test case presented above (the modified periodic vortex) with two different values for λ (*e.g.*, $\lambda_1 = 0.1$ and $\lambda_2 = 0.7$). The difference of the two velocity fields $\delta\hat{\boldsymbol{u}}$ should then be equal to $\epsilon^3\delta\boldsymbol{u}^{(3)}$ in leading order. If the prediction is correct, the field

$$\delta\hat{\boldsymbol{u}} - \epsilon^3\hat{\boldsymbol{w}} + \epsilon^3\delta\lambda\boldsymbol{G} \tag{33}$$

should then be of the order ϵ^5. Here, $\hat{\boldsymbol{w}}$ is any second order accurate solution of the $\boldsymbol{w}$ problem. We have calculated $\hat{\boldsymbol{w}}$ using the LB algorithm (24) with a modified equilibrium distribution where the quadratic part $F^{\mathrm{Q(eq)}}(\boldsymbol{u},\boldsymbol{u})$ is appropriately replaced by $F^{\mathrm{Q(eq)}}(\boldsymbol{u}^{(1)},\boldsymbol{w})$ with the exact solution $\boldsymbol{u}^{(1)}$ of the Navier-Stokes problem. Similarly, the corrected difference of densities

$$\delta\hat{\rho} - \epsilon^4\hat{q}/c_s^2 \tag{34}$$

should be of order ϵ^6. In Fig. 3, the expressions (33) and (34) computed from several grids is plotted *versus* the grid size in log-log scales. The slopes of the least squares fitted error curve are 4.93 for velocity and 6.65 for pressure which reflects the prediction of our asymptotic analysis.

7.   CONCLUSIONS

In this article we present a general methodology to conduct an order-by-order consistency analysis of the lattice Boltzmann equation. Our approach is based on
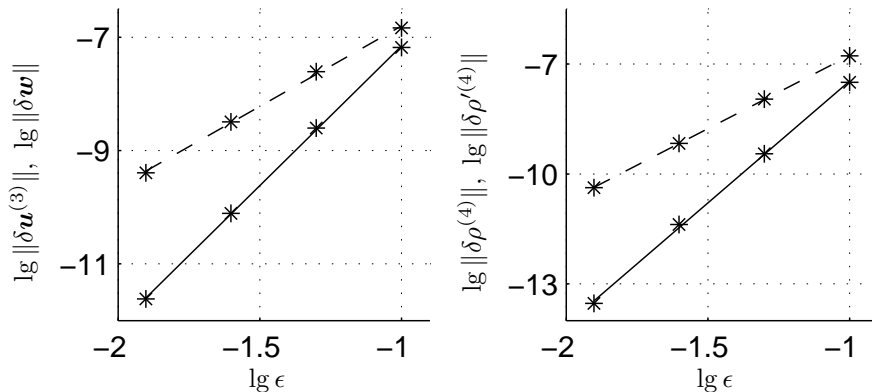
FIG. 3.   Left: ϵ-dependence of the maximum $\delta\boldsymbol{u}^{(3)}$ (dashed) and the maximum $\delta\boldsymbol{w} :=$ $\hat{\boldsymbol{w}} - \delta\lambda\boldsymbol{G}$ (solid). The least-square slopes are 2.84 and 4.93. Right: maximum of $\delta\rho^{(4)}$ (dashed) and of $\delta\rho'^{(4)} := \delta\rho^{(4)} - \epsilon^4\hat{q}$ (solid). The least-square slopes are 3.98 and 6.65.

a direct asymptotic analysis of finite difference schemes which is fairly general and has been widely used in numerical analysis. It turns out that the basic steps in the asymptotic expansion are parallel to the approach of Sone [43, 44] for the continuous Boltzmann equation and we highlight this particular relation by explicitly pointing out the connection between the LBE and a continuous FDVM. We demonstrate that the asymptotic analysis yields details about the accuracy of the lattice Boltzmann method and the structure of the error. The methodology presented here can be readily extended to analyze various boundary conditions, coupling conditions, and initial layers in the LBE simulations.

We would like to point out that the asymptotic analysis presented here in several aspects differs from the traditional Chapman-Enskog (CE) treatment of the lattice Boltzmann equation, which leads to the *compressible* Navier-Stokes equations. First, our approach uses a single time scale as opposed to the two-time-scale (multiple-time-scale in general) expansion in the CE analysis. Although it is easy to use two time-scales in the asymptotic analysis by simply setting

$$\hat{f}(n, \boldsymbol{j}, \boldsymbol{v}) = f^{(0)}(\epsilon n, \epsilon^2 n, \epsilon\boldsymbol{j}, \boldsymbol{v}) + \epsilon f^{(1)}(\epsilon n, \epsilon^2 n, \epsilon\boldsymbol{j}, \boldsymbol{v}) + \epsilon^2 f^{(2)}(\epsilon n, \epsilon^2 n, \epsilon\boldsymbol{j}, \boldsymbol{v}) + \ldots,$$

we do not do so for the following reason. The lattice Boltzmann equation is intended to solve the *incompressible* Navier-Stokes equation, therefore the relevant time scale is the slower one $t_n = \epsilon^2 n$. Within the context of incompressible Navier-Stokes equation, effects which occur in the faster time scale $\epsilon n = t_n/\epsilon$ (such as sound waves) are merely numerical effects. Were these effects indeed relevant in the leading orders of the flow velocity and pressure, then the LBE method is no longer valid for the purpose of simulating the incompressible Navier-Stokes equations and they are in fact beyond the realm of the *incompressible* Navier-Stokes equations. Hence, the validity of an expansion *regular* in the leading orders for the LBE solutions is *equivalent* to the validity of the LBE approximation for the *smooth* and *incompressible* Navier-Stokes solutions. In the same token, we also conclude that Knudsen-number effects observed in the LBE simulations are merely numerical

artifacts, because the effective Knudsen number Kn := ϵ is coupled with the discretization, *i.e.*, $\epsilon^2 = \Delta x^2 = \Delta t$, so that Knudsen-number effects are only observed on the grid scale (e.g., [8]). It is therefore incorrect to perceive these numerical artifacts in the LBE simulations as physical effects (*e.g.*, [32]) because, by its very nature, the lattice Boltzmann equation cannot capture the Knudsen layer. To analyze numerical Knudsen-number effects, a singular asymptotic expansion should be used [25]. We should stress that the ultimate goal of such an analysis is to mitigate artificial Knudsen-number effects by making them higher order one so to improve the smoothness of the numerical solution.

The second and significant difference between our approach and the CE analysis is in the structure of the expansion. In the CE analysis, it is assumed that the numerical solution can be written as

$$\hat{f} = F^{(\mathrm{eq})}(\rho, \boldsymbol{u}) + \epsilon g^{(1)} + \epsilon^2 g^{(2)} + \dots,$$

where ρ, $\boldsymbol{u}$ and $g^{(k)}$ are smooth functions which can be evaluated at the space-time grid points $(n, \boldsymbol{j})$. Furthermore, the functions $g^{(k)}$, $k = 1, 2, \dots$, are assumed to have no contribution to the conserved quantities (ρ and $\boldsymbol{u}$ here). Consequently, in the CE approach one must assume the existence of smooth functions ρ and $\boldsymbol{u}$ interpolating the averages $\hat{\rho}$ and $\hat{\boldsymbol{u}}$ of the LB solutions at the grid points. (A similar assumption forms the basis of the modified equation analysis which is criticized in [16, 5].) There are two undesirable consequences of this assumption. First, the smoothness assumption is generally not valid because the numerical solution typically exhibits irregular or non-smooth behavior in some order of ϵ. In our analysis this is not crucial because it is only the leading order quantities which are required to be smooth while higher order quantities may be irregular. And second, the smoothness assumption relies on the fact that the CE analysis is based on a given partial differential equation (the Boltzmann equation) for f from which a set of partial differential equations for the conserved quantities are derived subsequently. In the LBE method, ρ and $\boldsymbol{u}$ are determined by a *difference* equation, and there is no PDE to be satisfied by ρ and $\boldsymbol{u}$ *exactly*. It is only possible to show that ρ and $\boldsymbol{u}$ *approximately* satisfy certain PDEs in which the error terms depending on higher order derivatives of ρ and $\boldsymbol{u}$. By directly tackling the discrete lattice Boltzmann equation, our approach provides an order-by-order information about the structure of the LBE solution. In particular, the underlying incompressible Navier-Stokes problem emerges in this description so that it is straightforward to quantify the deviation from the exact solution of a target problem.

Apart from these conceptual differences, there is nevertheless a close connection between the asymptotic analysis and CE analysis. If in CE analysis the (hypothetical) functions ρ and $\boldsymbol{u}$ are expanded in terms of ϵ, one recovers equations for the expansion coefficients which are precisely those obtained directly with the asymptotic analysis. Conversely, a truncated expansion $\tilde{\boldsymbol{u}} = \boldsymbol{u}_0 + \epsilon \boldsymbol{u}_1 + \dots + \epsilon^m \boldsymbol{u}_m$ is given based on the coefficients constructed from the asymptotic analysis, then $\tilde{\boldsymbol{u}}$ differs from the CE moment $\boldsymbol{u}$ at most in the order ϵ^{m+1}, provided that the function $\boldsymbol{u}$ exists within the CE analysis.

Finally, we hope that with the new analytical method we can close a gap in the consistency analysis of the lattice Boltzmann equation. We also realize that

the method used in here can be applied to analyze other features like boundary conditions and initial layers in the lattice Boltzmann simulations. These are the subjects of our future study [4].

ACKNOWLEDGMENTS

APPENDIX A
ASYMPTOTIC ANALYSIS OF THE LBE

A.1. PRELIMINARY REMARKS

The analysis of both the FDVM and the LBE depends on certain algebraic properties of the collision operator. We summarize the key properties in a form which is convenient for the subsequent asymptotic expansion.

As before, we denote the orthogonal projection onto the kernel of A by Q so that the corresponding projector onto the orthogonal complement is

$$\mathsf{P} := \mathsf{I} - \mathsf{Q}.$$

That the mapping A is positive definite on the orthogonal complement of $\mathsf{Q}\mathcal{F}$ allows us to define its pseudo-inverse

$$\mathsf{A}^{\dagger} := \left(\mathsf{A}|_{\mathsf{P}(\mathcal{F})}\right)^{-1} \mathsf{P}.$$

Note that $\mathsf{A}^{\dagger} : \mathcal{F} \to \mathcal{F}$ has the property

$$\mathsf{A}\mathsf{A}^{\dagger} = \mathsf{P}$$

so that $\mathsf{A}^{\dagger}b$ solves the problem $\mathsf{A}z = b$, if $\mathsf{Q}b = 0$. This argument has been used in Sec. 4. The converse relation $\mathsf{A}^{\dagger}\mathsf{A} = \mathsf{P}$ yields together with $\mathsf{Q}[\Lambda f^*] = 0$ for the even function f^*, of which the lowest order moments have the same isotropy as the Maxwellian, and property (v)

$$\mathsf{A}^{\dagger}(\Lambda f^*) = \frac{\nu}{\kappa c_s^2}\Lambda f^*. \tag{A.1}$$

The assumed symmetry $\mathbb{V} = -\mathbb{V}$ of the velocity set implies that odd and even functions are orthogonal to each other. Introducing the odd and even projections for $f \in \mathcal{F}$:

$$(\mathsf{S}^+ f)(\boldsymbol{v}) = \frac{1}{2}[f(\boldsymbol{v}) + f(-\boldsymbol{v})], \qquad (\mathsf{S}^- f)(\boldsymbol{v}) = \frac{1}{2}[f(\boldsymbol{v}) - f(-\boldsymbol{v})],$$

we clearly have

$$\langle \mathsf{S}^- f, 1 \rangle = \frac{1}{2}\left(\sum_{\boldsymbol{c}\in\mathbb{V}} f(\boldsymbol{c}) - \sum_{\boldsymbol{c}\in-\mathbb{V}} f(\boldsymbol{c})\right) = 0$$

so that

$$\langle \mathsf{S}^- f, \mathsf{S}^+ g \rangle = \langle \mathsf{S}^-(f\mathsf{S}^+ g), 1 \rangle = 0, \qquad \forall f, g \in \mathcal{F}.$$

Using the projector S^-, the property of a function f to be even can be formulated as $\mathsf{S}^- f = 0$. For example, we have

$$\mathsf{S}^- f^{\mathrm{Q(eq)}}(f, g) = 0, \qquad \forall f, g \in \mathcal{F}, \tag{A.2}$$

Also property (iii) of the collision operator can be restated as $\mathsf{AS}^+ = \mathsf{S}^+\mathsf{A}$. One can also verify that Q commutes with S^+ so that the same carries over to P. Since $\mathsf{S}^- = \mathsf{I} - \mathsf{S}^+$, all the operators, A, $\mathsf{A}^\dagger$, Q and P commute with both the odd and even projections S^- and S^+.

A.2.   ANALYSIS OF THE FDVM

We exploit relations (18a), (18b) and (19) to determine the leading order coefficients $f^{(1)}$, $f^{(2)}$ and $f^{(3)}$. Starting with $k = -1$ and keeping in mind that $f^{(k)} = 0$ for $k < 0$, we conclude $f^{(1)} = f^{\mathrm{L(eq)}}(f^{(1)})$ from (19), *i.e.*,

$$f^{(1)} = \left(\rho^{(1)} + c_s^{-2} \boldsymbol{u}^{(1)} \cdot \mathbf{V} \right) f^*. \tag{A.3}$$

Equations (18a) and (18b) with $k = 0$ can further determine the moments $\rho^{(1)}$ and $\boldsymbol{u}^{(1)}$. Because $\rho^{(0)} = 1$ and $\boldsymbol{u}^{(0)} = \mathbf{0}$, and $\langle 1, \mathbf{V} \otimes \mathbf{V} f^{(1)} \rangle = c_s^2 \rho^{(1)} \mathsf{I}$, then

$$\boldsymbol{\nabla} \cdot \boldsymbol{u}^{(1)} = 0, \qquad \boldsymbol{\nabla} \rho^{(1)} = \mathbf{0}. \tag{A.4}$$

With $k = 1$, equations (18a) and (18b) will fully determine $\rho^{(1)}$ and $\boldsymbol{u}^{(1)}$ as the following. Based on equation (18a) and the fact that $\rho^{(1)}$ is $\boldsymbol{x}$-independent, the application of the divergence theorem to the integration over the periodic domain Ω leads to

$$\frac{d\rho^{(1)}}{dt} = \left(\int_\Omega d\boldsymbol{x} \right)^{-1} \int_\Omega \boldsymbol{\nabla} \cdot \boldsymbol{u}^{(2)} \, d\boldsymbol{x} = 0.$$

Since $\rho^{(1)} = 0$ initially [cf. equation (14a)], we conclude that $\rho^{(1)} = 0$ for all time $t \geq 0$. The final determination of $\boldsymbol{u}^{(1)}$ follows from (18b) with $k = 1$. However, in this equation, we need a scalar product involving the second expansion coefficient $f^{(2)}$ which we obtain again from (19)

$$f^{(2)} = f^{\mathrm{L(eq)}}(f^{(2)}) + f^{\mathrm{Q(eq)}}(f^{(1)}, f^{(1)}) - \mathsf{A}^\dagger(\mathbf{V} \cdot \boldsymbol{\nabla} f^{(1)}). \tag{A.5}$$

Using (A.3) with $\rho_1 = 0$, we find

$$\mathsf{A}^\dagger(\mathbf{V} \cdot \boldsymbol{\nabla} f^{(1)}) = c_s^{-2} \boldsymbol{\nabla} \boldsymbol{u}^{(1)} : \mathsf{A}^\dagger(\mathbf{V} \otimes \mathbf{V} f^*). \tag{A.6}$$

Since $\mathbf{V} \otimes \mathbf{V}$ is a symmetric matrix, we can replace the Jacobian $\boldsymbol{\nabla} \boldsymbol{u}^{(1)}$ by its symmetric part $\mathsf{S}[\boldsymbol{u}^{(1)}]/2$ without changing the :-product, where

$$\mathsf{S}^{(1)} := \mathsf{S}[\boldsymbol{u}^{(1)}] := \boldsymbol{\nabla} \boldsymbol{u}^{(1)} + [\boldsymbol{\nabla} \boldsymbol{u}^{(1)}]^\mathsf{T}.$$

Because the trace of $\mathsf{S}^{(1)}$ is $2\boldsymbol{\nabla}\cdot\boldsymbol{u}^{(1)}$, which vanishes due to the incompressibility condition, $\mathbf{V}\otimes\mathbf{V}$ can be replaced by its traceless part

$$\Lambda := \mathbf{V}\otimes\mathbf{V} - \frac{1}{d}\mathbf{V}\cdot\mathbf{V}\,\mathsf{I},$$

and therefore,

$$\mathsf{A}^{\dagger}(\mathbf{V}\cdot\boldsymbol{\nabla}f^{(1)}) = \frac{1}{2c_s^2}\mathsf{S}^{(1)} : \mathsf{A}^{\dagger}\Lambda f^*.$$

Property (A.1) now implies that

$$\frac{1}{2c_s^2}\mathsf{A}^{\dagger}\Lambda f^* = \frac{\nu}{2c_s^4\kappa}\Lambda f^*.$$

Thus, (A.5) turns into

$$f^{(2)} = f^{\mathrm{L(eq)}}(f^{(2)}) + f^{\mathrm{Q(eq)}}(f^{(1)}, f^{(1)}) - \frac{1}{2\kappa c_s^4}\nu\mathsf{S}^{(1)} : \Lambda f^*. \tag{A.7}$$

Now we can evaluate the moment $\mathsf{p}^{(2)} = \left\langle 1, \mathbf{V}\otimes\mathbf{V}f^{(2)}\right\rangle$ required in (18b) with $k = 1$. According to (9) and (11), we have

$$\left\langle 1, \mathbf{V}\otimes\mathbf{V}[f^{\mathrm{L(eq)}}(f^{(2)}) + f^{\mathrm{Q(eq)}}(f^{(1)}, f^{(1)})]\right\rangle = \boldsymbol{u}^{(1)}\otimes\boldsymbol{u}^{(1)} + c_s^2\rho^{(2)}\mathsf{I},$$

and because of (7c)

$$\left\langle 1, \mathrm{V}_\alpha\mathrm{V}_\beta\Lambda_{\gamma\delta}f^*\right\rangle = -\kappa c_s^4\left(\frac{2}{d}\delta_{\alpha\beta}\delta_{\gamma\delta} - \delta_{\alpha\gamma}\delta_{\beta\delta} - \delta_{\alpha\delta}\delta_{\beta\gamma}\right)$$

which implies, in connection with $\mathrm{tr}(\mathsf{S}^{(1)}) = 2\boldsymbol{\nabla}\cdot\boldsymbol{u}^{(1)} = 0$,

$$\left\langle 1, \mathrm{V}_\alpha\mathrm{V}_\beta\frac{\nu}{2\kappa c_s^4}(\Lambda f^*) : \mathsf{S}^{(1)}\right\rangle = \nu S_{\alpha\beta}^{(1)}.$$

Altogether, the required moment is

$$\mathsf{p}^{(2)} = \boldsymbol{u}^{(1)}\otimes\boldsymbol{u}^{(1)} + c_s^2\rho^{(2)}\mathsf{I} - \nu\mathsf{S}^{(1)}.$$

By setting $p^{(2)} = c_s^2\rho^{(2)}$ and $k = 1$ in (18b), we reach the result:

$$\begin{aligned} \boldsymbol{\nabla}\cdot\boldsymbol{u}^{(1)} &= 0, \\ \partial_t\boldsymbol{u}^{(1)} + \boldsymbol{\nabla}\cdot(\boldsymbol{u}^{(1)}\otimes\boldsymbol{u}^{(1)}) + \boldsymbol{\nabla}p^{(2)} &= \nu\boldsymbol{\nabla}^2\boldsymbol{u}^{(1)}, \\ \boldsymbol{u}^{(1)}|_{t=0} &= \bar{\boldsymbol{u}}. \end{aligned} \tag{A.8}$$

Hence, the leading order contribution of the velocity

$$\boldsymbol{u}_\epsilon = \left\langle 1, \mathbf{V}f_\epsilon\right\rangle = \epsilon\boldsymbol{u}^{(1)} + \dots$$

satisfies the incompressible Navier-Stokes equation and the first non-trivial order of the density

$$\rho_\epsilon = \left\langle 1, f_\epsilon\right\rangle = 1 + c_s^{-2}\epsilon^2 p^{(2)} + \dots$$

is determined as the associated pressure.

In the next step, we show that $\boldsymbol{u}^{(2)} = 0$ and $\rho^{(3)}$ vanish identically which relies only on the algebraic behavior of the Boltzmann equation under odd/even projections. Actually, the observation can be generalized to the statement

$$\boldsymbol{u}^{(2m)} = 0, \qquad \rho^{(2m+1)} = 0, \qquad m \geq 0. \tag{A.9}$$

We observe that $f^{(0)} = f^*$ is an even function and that $f^{(1)} = c_s^{-2}\boldsymbol{u}^{(1)} \cdot \mathbf{V}f^*$ is an odd function. In an induction argument, we therefore assume that, for $k \geq 0$ being an even index, the coefficient $f^{(k)}$ is an even and $f^{(k+1)}$ an odd function. Applying the odd projection S^- to (19), observing (A.2), and noting that ∂_t and $\mathsf{A}^\dagger$ commute with S^-, and that $\mathsf{S}^-(\mathbf{V}\cdot\boldsymbol{\nabla}) = (\mathbf{V}\cdot\boldsymbol{\nabla})\mathsf{S}^+$, we obtain

$$\mathsf{S}^- f^{(k+2)} = \mathsf{S}^- f^{\mathrm{L(eq)}}(f^{(k+2)}) - \mathsf{A}^\dagger(\partial_t \mathsf{S}^- f^{(k)} + \mathbf{V}\cdot\boldsymbol{\nabla}\mathsf{S}^+ f^{(k+1)}).$$

Due to the induction assumption, $\mathsf{S}^- f^{(k)} = \mathsf{S}^+ f^{(k+1)} = 0$. Taking the structure of $f^{\mathrm{L(eq)}}$ into account, we arrive at

$$\mathsf{S}^- f^{(k+2)} = c_s^{-2}\boldsymbol{u}^{(k+2)} \cdot \mathbf{V}f^*.$$

Similarly, an application of S^+ to (19) with k replaced by $k+1$ leads to a drastic simplification. Now, the quadratic terms vanish because the summation condition $n + m = k + 3$ implies that exactly one of the two indexes has to be even, and the distribution function with an even index has a vanishing average velocity. Only for the even index $k+2$ we do not know yet whether $\boldsymbol{u}^{(k+2)} = 0$. Hence,

$$\mathsf{S}^+ f^{(k+3)} = \rho^{(k+3)} f^* + 2f^{\mathrm{Q(eq)}}(f^{(1)}, f^{(k+2)}) - \mathsf{A}^\dagger(\mathbf{V}\cdot\boldsymbol{\nabla})\mathsf{S}^- f^{(k+2)}. \tag{A.10}$$

To fix the unknown coefficients $\boldsymbol{u}^{(k+2)}$ and $\rho^{(k+3)}$, we use again relations (18a) and (18b). Since $\rho^{(k+1)} = 0$, equation (18a) with k replaced by $k+1$ yields the incompressibility condition

$$\boldsymbol{\nabla}\cdot\boldsymbol{u}^{(k+2)} = 0.$$

Next, we use equation (18b) with k replaced by $k+2$. The required tensor

$$\mathsf{p}^{(k+3)} = \left\langle 1, \mathbf{V}\otimes\mathbf{V}f^{(k+3)} \right\rangle = \left\langle 1, \mathbf{V}\otimes\mathbf{V}\mathsf{S}^+ f^{(k+3)} \right\rangle$$

has essentially the same structure as $\mathsf{p}^{(2)}$ because $\mathsf{S}^+ f^{(k+3)}$ in (A.10) is structurally similar to $f^{(2)}$ in (A.5). Using similar arguments as in connection with $\mathsf{p}^{(2)}$, we thus obtain

$$\mathsf{p}^{(k+3)} = 2\boldsymbol{u}^{(1)} \otimes \boldsymbol{u}^{(k+2)} + c_s^2\rho^{(k+3)}\mathsf{I} - \nu\mathsf{S}^{(k+2)}$$

where $\mathsf{S}^{(k+2)} = [\boldsymbol{\nabla}\boldsymbol{u}^{(k+2)}] + [\boldsymbol{\nabla}\boldsymbol{u}^{(k+2)}]^\mathsf{T}$. Setting $p^{(k+3)} = c_s^2\rho^{(k+3)}$, we find a homogeneous Oseen problem

$$\boldsymbol{\nabla}\cdot\boldsymbol{u}^{(k+2)} = 0,$$
$$\partial_t\boldsymbol{u}^{(k+2)} + 2\boldsymbol{\nabla}\cdot(\boldsymbol{u}^{(1)}\otimes\boldsymbol{u}^{(k+2)}) + \boldsymbol{\nabla}p^{(k+3)} = \nu\boldsymbol{\nabla}^2\boldsymbol{u}^{(k+2)},$$
$$\boldsymbol{u}^{(k+2)}|_{t=0} = 0, \quad \rho^{(k+3)}|_{t=0} = 0,$$

which only has the zero solution so that (A.9) follows.

Finally, we would like to discuss the structure of the equations for the non-trivial coefficients $\boldsymbol{u}^{(k+1)}$ and $\rho^{(k+2)}$ with even index $k \geq 2$. The first observation is that $\boldsymbol{u}^{(k+1)}$ is generally not an incompressible field because (18a) implies

$$\boldsymbol{\nabla} \cdot \boldsymbol{u}^{(k+1)} = -\partial_t \rho^{(k)}. \tag{A.11}$$

(For example, the divergence of $\boldsymbol{u}^{(3)}$ is given by the temporal variation of the Navier-Stokes pressure $p^{(2)} = c_s^2 \rho^{(2)}$ in (A.8) which usually depends on space and time.) The time evolution of $\boldsymbol{u}^{(k+1)}$ is governed by (18b) with k replaced by $k+1$, for which we need $\mathsf{p}^{(k+2)} = \langle 1, \mathbf{V} \otimes \mathbf{V} f^{(k+2)} \rangle$. The explicit structure of $\mathsf{p}^{(k+2)}$ is increasingly complicated for increasing k because it involves derivatives of the coefficients $\boldsymbol{u}^{(1)}, \ldots, \boldsymbol{u}^{(k-1)}$, and $\rho^{(2)}, \ldots, \rho^{(k)}$, as well as multiple applications of $\mathsf{A}^\dagger$ which we cannot simplify in our general approach where we minimized our assumptions on A (to simplify the appearing expressions, the action of A on functions of the form $R f^*$, where R is a polynomial in $\boldsymbol{v}$, should be specified which is, of course, possible for a given collision operator). In the following, we will therefore combine all terms in a function $b^{(k)}$ which are independent of $\boldsymbol{u}^{(k+1)}$ and $\rho^{(k+2)}$ in (19). In particular, the only contribution of $\mathsf{A}^\dagger(\mathbf{V} \cdot \boldsymbol{\nabla} f^{(k+1)})$ which is not absorbed in $b^{(k)}$ is the term $c_s^{-2} \boldsymbol{\nabla} \boldsymbol{u}^{(k+1)} : \mathsf{A}^\dagger(\mathbf{V} \otimes \mathbf{V} f^*)$. Applying the same simplifications as in the case of equation (A.6), we arrive at

$$\frac{1}{c_s^2} \boldsymbol{\nabla} \boldsymbol{u}^{(k+1)} : \mathsf{A}^\dagger(\mathbf{V} \otimes \mathbf{V} f^*) = \frac{\nu}{2\kappa c_s^4} \mathsf{S}^{(k+1)} : \Lambda f^* + \frac{1}{d c_s^2} \boldsymbol{\nabla} \cdot \boldsymbol{u}^{(k+1)} \mathsf{A}^\dagger(|\mathbf{V}|^2 f^*), \tag{A.12}$$

where $\mathsf{S}^{(k+1)} = [\boldsymbol{\nabla} \boldsymbol{u}^{(k+1)}] + [\boldsymbol{\nabla} \boldsymbol{u}^{(k+1)}]^\mathsf{T}$. Note that $\boldsymbol{\nabla} \cdot \boldsymbol{u}^{(k+1)}$ generally does not vanish, but this fact will not change the nature of the resulting equation because, Eq. (A.11) shows that $\boldsymbol{\nabla} \cdot \boldsymbol{u}^{(k+1)}$ is a known quantity depending on the lower order coefficient $\partial_t \rho^{(k)}$. In particular, we can absorb the second term on the right hand side of (A.12) into the function $b^{(k)}$ and thus have

$$f^{(k+2)} = \rho^{(k+2)} f^* + 2 f^{\mathrm{Q(eq)}}(f^{(1)}, f^{(k+1)}) - \frac{\nu}{2\kappa c_s^4} \mathsf{S}^{(k+1)} : \Lambda f^* + b^{(k)}.$$

To obtain the evolution equation of $\boldsymbol{u}^{(k+1)}$, we need the $\mathbf{V} \otimes \mathbf{V}$ moment of $f^{(k+2)}$. Using the same calculations as for $\mathsf{p}^{(2)}$, observing that $\boldsymbol{\nabla} \cdot \boldsymbol{u}^{(k+1)} = -\partial_t \rho^{(k)}$, we find

$$\mathsf{p}^{(k+2)} = 2 \boldsymbol{u}^{(1)} \otimes \boldsymbol{u}^{(k+1)} + c_s^2 \rho^{(k+2)} \mathsf{I} - \nu \mathsf{S}^{(k+1)} + \frac{2\nu}{d} \partial_t \rho^{(k)} \mathsf{I} + \langle 1, \mathbf{V} \otimes \mathbf{V} b^{(k)} \rangle.$$

If we introduce $\boldsymbol{B}^{(k)}$ as the divergence of the last two terms which only involve lower order coefficients, we finally arrive at the Oseen type equation for the coefficients $\boldsymbol{u}^{(k+1)}$ and $p^{(k+2)} =: c_s^2 \rho^{(k+2)}$ with even indexes $k \geq 2$

$$\begin{aligned} &\boldsymbol{\nabla} \cdot \boldsymbol{u}^{(k+1)} = -\partial_t \rho^{(k)}, \\ &\partial_t \boldsymbol{u}^{(k+1)} + 2 \boldsymbol{\nabla} \cdot (\boldsymbol{u}^{(1)} \otimes \boldsymbol{u}^{(k+1)}) + \boldsymbol{\nabla} p^{(k+2)} = \nu \boldsymbol{\nabla}^2 \boldsymbol{u}^{(k+1)} + \boldsymbol{B}^{(k)}, \\ &\boldsymbol{u}^{(k+1)}|_{t=0} = 0, \quad \rho^{(k+2)}|_{t=0} = 0. \end{aligned} \tag{A.13}$$

Note that for the determination of $\boldsymbol{u}^{(k+1)}$ and $p^{(k+2)}$, the function $\boldsymbol{B}^{(k)}$ can be regarded as a given source term because it is derived from the coefficient functions which are already determined in the previous order of the expansion.

In summary, we have a complete picture of the asymptotic behavior: the density and velocity moments of the solution f_ϵ of (12) have the form

$$\boldsymbol{u}_\epsilon = \epsilon \boldsymbol{u}^{(1)} + \epsilon^3 \boldsymbol{u}^{(3)} + \epsilon^5 \boldsymbol{u}^{(5)} + \ldots$$
$$\rho_\epsilon = 1 + \epsilon^2 \rho^{(2)} + \epsilon^4 \rho^{(4)} + \epsilon^6 \rho^{(6)} + \ldots.$$

where $\boldsymbol{u}^{(1)}$ and $c_s^2 \rho^{(2)}$ solve the Navier-Stokes equations and $\boldsymbol{u}^{(k+1)}$ and $\rho^{(k+2)}$, with $k = 2n \geq 2$, solve systems of type (A.13).

A.3.   ANALYSIS OF THE LBE

For $k = -1$ and $k = 0$, equations (30a), (30b) and (31) coincide with the counterparts in Sec. 4 because all space and time derivatives of $f^{(0)} = f^*$ vanish, $f^{(-1)} = 0$, and $L^{(0)} = L^{(1)} = 0$. We thus conclude

$$f^{(1)} = \left(\rho^{(1)} + c_s^{-2} \boldsymbol{u}^{(1)} \cdot \mathbf{V} \right) f^* \tag{A.14}$$

with

$$\boldsymbol{\nabla} \rho^{(1)} = 0, \qquad \boldsymbol{\nabla} \cdot \boldsymbol{u}^{(1)} = 0.$$

To show that even $\rho^{(1)} = 0$, we need (30a) with $k = 1$. Noting that $\mathsf{p}^{(1)} = c_s^2 \rho^{(1)} \mathsf{I}$ and $L^{(3)} = g$, we find

$$\partial_t \rho^{(1)} + \boldsymbol{\nabla} \cdot \boldsymbol{u}^{(2)} + \frac{1}{2} c_s^2 \boldsymbol{\nabla}^2 \rho^{(1)} = \langle 1, g \rangle.$$

Since $\boldsymbol{\nabla} \rho^{(1)} = 0$, the Laplacian $\boldsymbol{\nabla}^2 \rho^{(1)}$ also vanishes. Moreover, $\langle 1, g \rangle = 0$ because g is an odd function in $\boldsymbol{v}$. Therefore, in the case $k = 1$, (30a) coincides with (18a) and we conclude as in Sec. A.2 that $\rho^{(1)} = 0$ and

$$f^{(2)} = f^{\mathrm{L(eq)}}(f^{(2)}) + f^{\mathrm{Q(eq)}}(f^{(1)}, f^{(1)}) - \frac{\nu}{2\kappa c_s^4} \mathsf{S}^{(1)} : \Lambda f^*. \tag{A.15}$$

with the associated second moment

$$\mathsf{p}^{(2)} = \boldsymbol{u}^{(1)} \otimes \boldsymbol{u}^{(1)} + c_s^2 \rho^{(2)} \mathsf{I} - \nu S^{(1)}$$

which is needed in (30b) with $k = 1$ to derive the evolution equation for $\boldsymbol{u}^{(1)}$. Now, the right hand side $\boldsymbol{G} = \langle 1, \mathbf{V} g \rangle$ can be non-zero and acts as a force field in the equation for $\boldsymbol{u}^{(1)}$. The remaining term involving the second derivative of $f^{(1)}$ is anti-diffusive in nature. We have with (A.14) and $\rho^{(1)} = 0$

$$\left\langle 1, \mathrm{V}_\alpha (\mathbf{V} \cdot \boldsymbol{\nabla})^2 f^{(1)} \right\rangle = c_s^{-2} \left\langle 1, \mathrm{V}_\alpha \mathrm{V}_\beta \mathrm{V}_\gamma \mathrm{V}_\delta f^* \right\rangle \partial_\gamma \partial_\delta u_\beta^{(1)}.$$

Using (7c), we obtain

$$\left\langle 1, \mathrm{V}_\alpha (\mathbf{V} \cdot \boldsymbol{\nabla})^2 f^{(1)} \right\rangle = \kappa c_s^2 (\boldsymbol{\nabla}^2 u_\alpha^{(1)} + 2 \partial_\alpha \boldsymbol{\nabla} \cdot \boldsymbol{u}^{(1)}) = \kappa c_s^2 \boldsymbol{\nabla}^2 \boldsymbol{u}^{(1)}.$$

Combining these calculations, we see that $\boldsymbol{u}^{(1)}$ and $p^{(2)} = c_s^2 \rho^{(2)}$ satisfy an incompressible Navier-Stokes problem with the well known viscosity correction

$$\boldsymbol{\nabla}\cdot\boldsymbol{u}^{(1)} = 0,$$

$$\partial_t \boldsymbol{u}^{(1)} + \boldsymbol{\nabla}\cdot(\boldsymbol{u}^{(1)} \otimes \boldsymbol{u}^{(1)}) + \boldsymbol{\nabla}p^{(2)} = (\nu - \frac{1}{2}\kappa c_s^2)\boldsymbol{\nabla}^2 \boldsymbol{u}^{(1)} + \boldsymbol{G}, \qquad \text{(A.16)}$$

$$\boldsymbol{u}^{(1)}|_{t=0} = \bar{\boldsymbol{u}}.$$

To determine the higher order terms, we proceed as in Appendix. A.2 and show that $f^{(m)}$ is odd (even) if the index m is odd (even). In fact, the induction proof can essentially be taken over because of the odd/even symmetries of the additional terms $\frac{1}{2}(\mathbf{V}\cdot\boldsymbol{\nabla})^2 f^{(k)} + L^{(k+2)}$. Let us adopt the induction assumption that, for k even, $f^{(0)}, f^{(2)}, \ldots, f^{(k)}$ are even and $f^{(1)}, f^{(3)}, \ldots, f^{(k+1)}$ are odd. Then

$$L^{(k+2)} = g^{(k+2)} - \sum_{\substack{m+r=k+2 \\ m<k}} D_r(\partial_t, \mathbf{V}\cdot\boldsymbol{\nabla}) f^{(m)}$$

is even because $m + r = k + 2$ can only be even if both m and r are even and since $D_r(\partial_t, \mathbf{V}\cdot\boldsymbol{\nabla})$ is an even polynomial in $\mathbf{V}$, each term $D_r f^{(m)}$ in the sum is even. Combined with the even symmetry of $g^{(k+2)}$, we conclude $\mathsf{S}^- L^{(k+2)} = 0$. Similarly, we have $\mathsf{S}^+ L^{(k+3)} = 0 = \mathsf{S}^- L^{(k+4)}$ and, of course, $\mathsf{S}^-(\mathbf{V}\cdot\boldsymbol{\nabla})^2 f^{(k)} = 0 = \mathsf{S}^+(\mathbf{V}\cdot\boldsymbol{\nabla})^2 f^{(k+1)}$. With the same argument presented in Sec. A.2, we can show that $\boldsymbol{u}^{(k+2)}$ and $p^{(k+3)} = c_s^2 \rho^{(k+3)}$ satisfy the homogeneous Oseen problem

$$\boldsymbol{\nabla}\cdot\boldsymbol{u}^{(k+2)} = 0,$$

$$\partial_t \boldsymbol{u}^{(k+2)} + 2\boldsymbol{\nabla}\cdot(\boldsymbol{u}^{(1)} \otimes \boldsymbol{u}^{(k+2)}) + \boldsymbol{\nabla}p^{(k+3)} = (\nu - \frac{1}{2}\kappa c_s^2)\boldsymbol{\nabla}^2 \boldsymbol{u}^{(k+2)},$$

$$\boldsymbol{u}^{(k+2)}|_{t=0} = 0, \quad \rho^{(k+3)}|_{t=0} = 0,$$

where the modified viscosity appears because of $\langle 1, \mathbf{V}(\mathbf{V}\cdot\boldsymbol{\nabla})^2 f^{(k+2)} \rangle / 2$ in (30b) with k replaced by $k + 2$. Since the homogeneous Oseen problem has only the trivial solution $\boldsymbol{u}^{(k+2)} = 0$ and $p^{(k+3)} = 0$, we have $\mathsf{S}^- f^{(k+2)} = 0 = \mathsf{S}^+ f^{(k+3)}$ which concludes the induction proof.

To complete the analysis, we also derive the equations for the non-trivial fields $\boldsymbol{u}^{(k+1)}$ and $\rho^{(k+2)}$ with even $k \geq 2$. Now the divergence condition has additional source terms. From (30a), we find

$$\boldsymbol{\nabla}\cdot\boldsymbol{u}^{(k+1)} = \left\langle 1, L^{(k+2)} \right\rangle - \partial_t \rho^{(k)} - \frac{1}{2}\boldsymbol{\nabla}\otimes\boldsymbol{\nabla} : \mathsf{p}^{(k)}.$$

Finally, the evolution equation for $\boldsymbol{u}^{(k+1)}$ is obtained from (30b) with k replaced by $k + 1$. The required tensor $\mathsf{p}^{(k+2)}$ can be calculated by taking second moments of (31) which involves derivatives of lower order coefficients and multiple applications of $\mathsf{A}^\dagger$. If we collect all terms containing expressions with $\rho^{(2)}, \ldots, \rho^{(k)}$ and $\boldsymbol{u}^{(1)}, \ldots, \boldsymbol{u}^{(k-1)}$ as well as the given source g in a function $c^{(k)}$, we find as in Sec. A.2 that

$$f^{(k+2)} = \rho^{(k+2)} f^* + 2f^{\mathrm{Q(eq)}}(f^{(1)}, f^{(k+1)}) - \frac{\nu}{2\kappa c_s^4}\mathsf{S}^{(k+1)} : \Lambda f^* + c^{(k)}.$$

and from (30b), we finally get the Oseen type equation

$$\boldsymbol{\nabla} \cdot \boldsymbol{u}^{(k+1)} = \left\langle 1, L^{(k+2)} \right\rangle - \partial_t \rho^{(k)} - \frac{1}{2} \boldsymbol{\nabla} \otimes \boldsymbol{\nabla} : \mathsf{p}^{(k)},$$

$$\partial_t \boldsymbol{u}^{(k+1)} + 2\boldsymbol{\nabla} \cdot (\boldsymbol{u}^{(1)} \otimes \boldsymbol{u}^{(k+1)}) + \boldsymbol{\nabla} p^{(k+2)} = (\nu - \frac{1}{2}\kappa c_s^2)\boldsymbol{\nabla}^2 \boldsymbol{u}^{(k+1)} + \boldsymbol{C}^{(k)}, \quad \text{(A.17)}$$

$$\boldsymbol{u}^{(k+1)}|_{t=0} = 0, \quad \rho^{(k+2)}|_{t=0} = 0.$$

Here $\boldsymbol{C}^{(k)}$ contains all lower order and force terms which appear when calculating the required $\mathbf{V} \otimes \mathbf{V}$ moments like $\left\langle 1, \mathbf{V} \otimes \mathbf{V} c^{(k)} \right\rangle$ but also the terms which involving $\boldsymbol{\nabla} \cdot \boldsymbol{u}^{(k+1)}$ which depends only on lower order and force terms because of (30a).

A.4.   EFFECTS OF THE PARAMETER λ

In this section, we investigate how two numerical solutions differ in leading order if two different parameters λ_1 and λ_2 are used in the scheme (24). We denote the expansion coefficients in the two cases by $f^{(m,\lambda_1)}$, $f^{(m,\lambda_2)}$, and their difference is defined as

$$\delta f^{(m)} = f^{(m,\lambda_1)} - f^{(m,\lambda_2)}.$$

Similar notation is applied to the velocity moments. In light of (A.14) and (A.15), the first two expansion coefficients are independent of λ, so that

$$\delta f^{(1)} = \delta f^{(2)} = 0 \tag{A.18}$$

and we can simply refer to $f^{(1)}$ and $f^{(2)}$ instead of $f^{(1,\lambda)}$ and $f^{(2,\lambda)}$. Before we derive $\delta f^{(3)}$ and $\delta f^{(4)}$, we consider the terms $L^{(m,\lambda)}$ defined in (29) up to $m = 5$. We have

$$\delta L^{(0)} = \delta L^{(1)} = \delta L^{(2)} = \delta L^{(3)} = 0$$

and since $L^{(4,\lambda)}$ depends only on $f^{(1)}$ apart from $g^{(4,\lambda)} = (1-\lambda)(\mathbf{V} \cdot \boldsymbol{\nabla})g$,

$$\delta L^{(4)} = -\delta\lambda(\mathbf{V} \cdot \boldsymbol{\nabla})g, \qquad \delta\lambda = \lambda_1 - \lambda_2. \tag{A.19}$$

Similarly, $L^{(5,\lambda)}$ only depends on $f^{(1)}$, $f^{(2)}$ and $g^{(5,\lambda)}$, so that because of (A.18)

$$\delta L^{(5)} = -\delta\lambda \left(\partial_t g + \frac{1}{2}(\mathbf{V} \cdot \boldsymbol{\nabla})^2 g \right) \tag{A.20}$$

Coming back to the coefficients $f^{(m,\lambda)}$, we observe from (31) with $k = 1$ that

$$\delta f^{(3)} = c_s^{-2}\delta\boldsymbol{u}^{(3)} \cdot \mathbf{V} f^* \tag{A.21}$$

where we have used (A.18) and $\rho^{(3)} = 0$, $\delta L^{(3)} = 0$. Similarly, with $k = 2$, we find

$$\delta f^{(4)} = \delta\rho^{(4)} f^* + 2f^{Q(\mathrm{eq})}(f^{(1)}, \delta f^{(3)}) - \mathsf{A}^\dagger(\mathbf{V} \cdot \boldsymbol{\nabla})\delta f^{(3)} + \mathsf{A}^\dagger\delta L^{(4)}.$$

The BGK assumption allows to replace $\mathsf{A}^\dagger$ by $(\nu/\kappa c_s^2)\mathsf{I}$ and in view of (A.19), (32), and (A.21), we can write more explicitly

$$\delta f^{(4)} = \delta\rho^{(4)} f^* + 2f^{Q(\mathrm{eq})}(f^{(1)}, \delta f^{(3)}) - \frac{\nu}{\kappa c_s^4}(\mathbf{V} \otimes \mathbf{V})f^* : \boldsymbol{\nabla}\boldsymbol{w} \tag{A.22}$$

where we introduce

$$\boldsymbol{w} = \delta\boldsymbol{u}^{(3)} + \delta\lambda\boldsymbol{G}. \tag{A.23}$$

The evolution equation for $\delta\boldsymbol{u}^{(3)}, \delta\rho^{(4)}$ follows from (30a) and (30b) by taking differences and observing that $\delta f^{(2)} = 0$.

$$\boldsymbol{\nabla}\cdot\delta\boldsymbol{u}^{(3)} = \left\langle 1, \delta L^{(4)}\right\rangle \tag{A.24}$$

$$\partial_t \boldsymbol{u}^{(3)} + \boldsymbol{\nabla}\cdot\mathsf{p}^{(4)} + \frac{1}{2}\left\langle 1, \mathbf{V}(\mathbf{V}\cdot\boldsymbol{\nabla})^2 f^{(3)}\right\rangle = \left\langle 1, \mathbf{V}L^{(5)}\right\rangle. \tag{A.25}$$

Using (A.19) and (32), we find $\left\langle 1, \delta L^{(4)}\right\rangle = -\delta\lambda\boldsymbol{\nabla}\cdot\boldsymbol{G}$, so that the first condition reduces to a divergence-free condition for the field (A.23)

$$\boldsymbol{\nabla}\cdot\boldsymbol{w} = 0.$$

To evaluate (A.25), we first consider the $\delta L^{(5)}$ term

$$\left\langle 1, \mathbf{V}L^{(5)}\right\rangle = -\frac{\delta\lambda}{c_s^2}\left\langle 1, \mathbf{V}\otimes\mathbf{V}f^*\right\rangle\partial_t\boldsymbol{G} - \frac{\delta\lambda}{2c_s^2}\left\langle 1, \mathbf{V}(\mathbf{V}\cdot\boldsymbol{\nabla})^2\boldsymbol{G}\cdot\mathbf{V}f^*\right\rangle$$

which can be combined with the $\delta f^{(3)}$ term in (A.25)

$$\left\langle 1, \mathbf{V}L^{(5)}\right\rangle - \frac{1}{2}\left\langle 1, \mathbf{V}(\mathbf{V}\cdot\boldsymbol{\nabla})^2 f^{(3)}\right\rangle = -\delta\lambda\partial_t\boldsymbol{G} - \frac{1}{2c_s^2}\left\langle 1, \mathbf{V}(\mathbf{V}\cdot\boldsymbol{\nabla})^2\boldsymbol{w}\cdot\mathbf{V}f^*\right\rangle$$

and using $\boldsymbol{\nabla}\cdot\boldsymbol{w} = 0$ we calculate with (7c)

$$\left\langle 1, \mathbf{V}L^{(5)}\right\rangle - \frac{1}{2}\left\langle 1, \mathbf{V}(\mathbf{V}\cdot\boldsymbol{\nabla})^2 f^{(3)}\right\rangle = -\delta\lambda\partial_t\boldsymbol{G} - \frac{\kappa c_s^2}{2}\Delta\boldsymbol{w}$$

Finally, the $\delta\mathsf{p}^{(4)}$ contribution is calculated from (A.22)

$$\delta\mathsf{p}^{(4)} = c_s^2\delta\rho^{(4)}\mathsf{I} + 2\boldsymbol{u}^{(1)}\otimes\delta\boldsymbol{u}^{(3)} - \nu\delta\mathsf{S}^{(3)} - \nu\mathsf{S}[\boldsymbol{w}].$$

Altogether, the equation for $\boldsymbol{w} = \delta\boldsymbol{u}^{(3)} + \delta\lambda\boldsymbol{G}$ and $q = c_s^2\delta\rho^{(4)}$ reads

$$\boldsymbol{\nabla}\cdot\boldsymbol{w} = 0,$$

$$\partial_t\boldsymbol{w} + 2\boldsymbol{\nabla}\cdot(\boldsymbol{u}^{(1)}\otimes\boldsymbol{w}) + \boldsymbol{\nabla}q = (\nu - \frac{1}{2}\kappa c_s^2)\boldsymbol{\nabla}^2\boldsymbol{w} + 2\delta\lambda\boldsymbol{\nabla}\cdot(\boldsymbol{u}^{(1)}\otimes\boldsymbol{G}),$$

$$\boldsymbol{w}|_{t=0} = 0, \quad q|_{t=0} = 0,$$

APPENDIX B
THE LBE MODELS

B.1.   THE D2Q9 MODEL

In the D2Q9 model, the velocities are $\mathbb{V} = \{\boldsymbol{c}_0, \boldsymbol{c}_1, \ldots, \boldsymbol{c}_8\}$ with $\boldsymbol{c}_0 = \boldsymbol{0}$ and

$$\boldsymbol{c}_1 = \begin{pmatrix}1\\0\end{pmatrix} \qquad \boldsymbol{c}_2 = \begin{pmatrix}0\\1\end{pmatrix} \qquad \boldsymbol{c}_3 = \begin{pmatrix}-1\\0\end{pmatrix} \qquad \boldsymbol{c}_4 = \begin{pmatrix}0\\-1\end{pmatrix}$$
$$\boldsymbol{c}_5 = \begin{pmatrix}1\\1\end{pmatrix} \qquad \boldsymbol{c}_6 = \begin{pmatrix}-1\\1\end{pmatrix} \qquad \boldsymbol{c}_7 = \begin{pmatrix}-1\\-1\end{pmatrix} \qquad \boldsymbol{c}_8 = \begin{pmatrix}1\\-1\end{pmatrix}$$

The function f^* is defined in terms of the weights

$$f^*(\mathbf{c}_i) = \begin{cases} 4/9, & i = 0, \\ 1/9, & i = 1, 2, 3, 4, \\ 1/36, & i = 5, 6, 7, 8 \end{cases}$$

which implies $c_s^2 = 1/3$ in (7b) and $\kappa = 1$ in (7c). The construction of the equilibrium distribution described in Sec. 3.2 then gives rise to the function defined in [17],

$$F^{(\mathrm{eq})}(\rho, \boldsymbol{u};\, \boldsymbol{v}) = \left[\rho + \bar{\rho}\left(3\boldsymbol{u}\cdot\boldsymbol{v} + \frac{3}{2}(\boldsymbol{u}\cdot\boldsymbol{v})^2 - \frac{3}{2}|\boldsymbol{u}|^2\right)\right] f^*(\boldsymbol{v}), \qquad \bar{\rho} \equiv 1.$$

A large class of operators A satisfying the criteria (i) to (v) listed in Sec. 3.2 can be constructed using an orthonormal basis $\{\varphi_1, \ldots, \varphi_9\}$ of $\mathcal{F}$ given by [10]

$$\varphi_1(\boldsymbol{v}) = \tfrac{1}{3},$$
$$\left.\begin{aligned} \varphi_2(\boldsymbol{v}) &= \tfrac{1}{\sqrt{6}}v_x, \\ \varphi_3(\boldsymbol{v}) &= \tfrac{1}{\sqrt{6}}v_y, \end{aligned}\right\}$$
$$\left.\begin{aligned} \varphi_4(\boldsymbol{v}) &= \tfrac{1}{2}v_x v_y, \\ \varphi_5(\boldsymbol{v}) &= \tfrac{1}{2}(v_x^2 - v_y^2), \\ \varphi_6(\boldsymbol{v}) &= \tfrac{1}{6}(4 - 3\boldsymbol{v}^2), \end{aligned}\right\}$$
$$\left.\begin{aligned} \varphi_7(\boldsymbol{v}) &= \tfrac{\sqrt{3}}{6}v_x(2 - 3v_y^2), \\ \varphi_8(\boldsymbol{v}) &= \tfrac{\sqrt{3}}{6}v_y(2 - 3v_x^2), \end{aligned}\right\}$$
$$\varphi_9(\boldsymbol{v}) = \tfrac{3}{2}(v_x^2 v_y^2 + 1) - \boldsymbol{v}^2.$$

Using the orthogonal projectors $\mathsf{Q}_i f = \langle f, \varphi_i\rangle \varphi_i$, we obtain a class of linear operators

$$\mathsf{A} = \sum_{i=1}^{9} \lambda_i \mathsf{Q}_i,$$

which satisfy the required conditions (i) to (v) under certain conditions on the eigenvalues λ_i. For example, condition (ii) can be achieved with $\lambda_i \geq 0$ while (i) follows from the fact that each Q_i is self-adjoint. Since each φ_i is either odd or even, the subspaces of odd and even functions are invariant subspaces of A and hence $\mathsf{A}\mathsf{S}^+ = \mathsf{S}^+\mathsf{A}$. The condition (iv) on the kernel of A follows with $\lambda_1 = \lambda_2 = \lambda_3 = 0$ and, in view of the fact that $\mathsf{\Lambda}f^*$ can be expressed in terms of φ_4, φ_5, we set $\lambda_4 = \lambda_5 = c_s^2\nu$ in order to satisfy (v). Altogether, the conditions on A hold with

$$\lambda_1 = \lambda_2 = \lambda_3 = 0,$$
$$\lambda_4 = \lambda_5 = c_s^2\nu,$$
$$\lambda_6, \ldots, \lambda_9 > 0.$$

B.2. THREE-DIMENSIONAL MODELS

For the models D3Q15 and D3Q19, details about velocities c_i and weights f_i^* can be found, for example, in [36]. In each case, we have $\kappa = 1$ and $c_s^2 = 1/3$ so that the equilibrium distribution has the same structure as in the previous section. Using the orthogonal polynomials for these models presented in [11], we can again set up A using the orthogonal projections. With the numbering of the polynomials given in [11], we have to set

$$\lambda_0 = \lambda_3 = \lambda_5 = \lambda_7 = 0,$$
$$\lambda_9 = \cdots = \lambda_{13} = c_s^2 \nu,$$
$$\lambda_1, \lambda_2, \lambda_4, \lambda_6, \lambda_8, \lambda_{14} > 0$$

for the D3Q15 model, and

$$\lambda_0 = \lambda_3 = \lambda_5 = \lambda_7 = 0,$$
$$\lambda_9 = \cdots = \lambda_{15} = c_s^2 \nu,$$
$$\lambda_1, \lambda_2, \lambda_4, \lambda_6, \lambda_8, \lambda_{16}, \lambda_{17}, \lambda_{18} > 0$$

in the D3Q19 case.

REFERENCES

1. C. Bardos, F. Golse, and D. Levermore. Fluid dynamic limits of kinetic equations: Formal derivations. *J. Stat. Phys.*, 63:323–344, 1991.

2. R. Benzi, S. Succi, and M. Vergassola. The lattice-Boltzmann equation: Theory and applications. *Phys. Rep.*, 222:145–197, 1992.

3. P.L. Bhatnagar, E.P. Gross, and M. Krook. A model for collision processes in gases I: Small amplitude processes in charged and neutral one-component systems. *Phys. Rev.*, 94:511–525, 1954.

4. A. Caiazzo. Analysis of lattice Boltzmann initialization routines. To appear in J. Stat. Phys., 2005.

5. S.-C. Chang. A critical analysis of the modified equation technique of Warming and Hyett. *J. Comput. Phys.*, 86:107–126, 1990.

6. H. Chen, S. Chen, and W. Matthaeus. Recovery of the Navier-Stokes equations using a lattice-gas Boltzmann method. *Phys. Rev. A*, 45:5339–5342, 1992.

7. S. Chen and G.D. Doolen. Lattice Boltzmann method for fluid flows. *Annu. Rev. Fluid Mech.*, 30:329–364, 1998.

8. R. Cornubert, D. d'Humières, and C.D. Levermore. A Knudsen layer theory for lattice gases. *Physica D*, 47:241–259, 1991.

9. A. De Masi, R. Esposito, and J.L. Lebowitz. Incompressible Navier-Stokes and Euler limits of the Boltzmann equation. *Comm. Pure Applied Math.*, 42:1189, 1989.

10. D. d'Humières. Generalized lattice-Boltzmann equations. In D. Shizgal and D.P. Weaver, editors, *Rarefied Gas Dynamics: Theory and Applications*, volume 159 of *Progress in Astronautics and Aeoronautics*, pages 450–458, Washington D.C., 1992. AIAA.

11. D. d'Humières, I. Ginzburg, M. Krafczyk, P. Lallemand, and L.-S. Luo. Multiple-relaxation-time lattice Boltzmann models in three dimensions. *Philos. Trans. R. Soc. Lond. A*, 360:437–451, 2002.

12. U. Frisch, D. d'Humières, B. Hasslacher, P. Lallemand, Y. Pomeau, and J.P. Rivet. Lattice gas hydrodynamics in two and three dimensions. *Complex Systems*, 1:649–707, 1987.

13. U. Frisch, B. Hasslacher, and Y. Pomeau. Lattice-gas automata for the Navier-Stokes equation. *Phys. Rev. Lett.*, 56:1505–1508, 1986.

14. F. Golse and L. Saint-Raymond. The Navier-Stokes limit of the Boltzmann equation. *C. R. Acad. Sci. Paris Série I*, 333(9):897–902, 2001.

15. F. Golse and L. Saint-Raymond. The Navier-Stokes limit of the Boltzmann equation for bounded collision kernels. *Invent. Math.*, 155:81–161, 2004.

16. D.F. Griffiths and J.M. Sanz-Serna. On the scope of the method of modified equations. *SIAM J. Sci. Stat. Comput.*, 7:994–1008, 1986.

17. X. He and L.-S. Luo. Lattice Boltzmann model for the incompressible Navier-Stokes equation. *J. Stat. Phys.*, 88:927–944, 1997.

18. X. He and L.-S. Luo. A priori derivation of the lattice Boltzmann equation. *Phys. Rev. E*, 55:6333–6336, 1997.

19. X. He and L.-S. Luo. Theory of the lattice Boltzmann method: From the Boltzmann equation to the lattice Boltzmann equation. *Phys. Rev. E*, 56:6811–6817, 1997.

20. F.J. Higuera and J. Jiménez. Boltzmann approach to lattice gas simulations. *Europhys. Lett.*, 9:663–668, 1989.

21. F.J. Higuera, S. Succi, and R. Benzi. Lattice gas dynamics with enhanced collisions. *Europhys. Lett.*, 9:345–349, 1989.

22. A. Ilachinski. *Cellular Automata*. World Scientific, Singapore, 2001.

23. T. Inamuro, M. Yoshino, and F. Ogino. Accuracy of the lattice Boltzmann method for small Knudsen number with finite Reynolds number. *Phys. Fluids*, 9:3535–3542, 1997.

24. M. Junk. A finite difference interpretation of the lattice Boltzmann method. *Numer. Methods Partial Differ. Equations*, 17:383–402, 2001.

25. M. Junk and Z. Yang. Analysis of lattice Boltzmann boundary conditions. *Proc. Appl. Math. Mech.*, 3:76–79, 2003.

26. M. Junk and Z. Yang. Asymptotic analysis of finite difference methods. *To appear in Appl. Math. Computat.*, 2005.

27. M. Junk and W.A. Yong. Rigorous Navier-Stokes limit of the lattice Boltzmann equation. *Asymptotic Analysis*, 35:165–185, 2003.

28. P. Lallemand and L.-S. Luo. Theory of the lattice Boltzmann method: Dispersion, dissipation, isotropy, Galilean invariance, and stability. *Phys. Rev. E*, 61:6546–6562, 2000.

29. P.-L. Lions and M. Masmoudi. From the Boltzmann equations to the equations of incompressible fluid mechanics: Part I and II. *Arch. Rational Mech. Anal.*, 158:173–211, 2001.

30. L.-S. Luo. Unified theory of the lattice Boltzmann models for nonideal gases. *Phys. Rev. Lett.*, 81:1618–1621, 1998.

31. L.-S. Luo. Theory of the lattice Boltzmann method: Lattice Boltzmann models for nonideal gases. *Phys. Rev. E*, 62:4982–4996, 2000.

32. L.-S. Luo. Comment on "Discrete Boltzmann equation for microfluidics". *Phys. Rev. Lett.*, 92:139401, 2004.

33. G.I. Marchuk and V.V. Shaidurov. *Difference methods and their extrapolations*. Springer, 1983.

34. N.S. Martys, X. Shan, and H. Chen. Evaluation of the external force term in the discrete Boltzmann equation. *Physical Review E*, 58:6855–6857, 1998.

35. G. R. McNamara and G. Zanetti. Use of the Boltzmann equation to simulate lattice-gas automata. *Phys. Rev. Lett.*, 61:2332–2335, 1988.

36. R. Mei, W. Shyy, D. Yu, and L.S. Luo. Lattice Boltzmann method for 3-d flows with curved boundary. *J. Comp. Phys.*, 161:680–699, 2000.

37. C. Pan, L.-S. Luo, and C. T. Miller. An evaluation of lattice Boltzmann schemes for porous medium flow simulation. To appear in Comput. Fluid, 2005.

38. D. Qi and L.-S. Luo. Transitions in rotations of a nonspherical particle in a three-dimensional moderate Reynolds number Couette flow. *Phys. Fluid*, 14:4440–4443, 2002.

39. D. Qi and L.-S. Luo. Rotational and orientational behaviour of a three-dimensional spheroidal particles in Couette flow. *J. Fluid Mech.*, 477:201–213, 2003.

40. D. Qi, L.-S. Luo, R. Aravamuthan, and W. Strieder. Lateral migration and orientation of elliptical particles in Poiseuille flows. *J. Stat. Phys.*, 107:102–120, 2002.

41. Y.H. Qian, D. d'Humières, and P. Lallemand. Lattice BGK models for the Navier-Stokes equation. *Europhys. Lett.*, 17:479–484, 1992.

42. M. Rheinländer. A consistent grid coupling method for lattice-Boltzmann schemes. to appear in J. Stat. Phys., 2005.

43. Y. Sone. Asymptotic theory of a steady flow of a rarefied gas past bodies for small Knudsen numbers. In R. Gatignol and J.B. Soubbaramayer, editors, *Advances in Kinetic Theory and Continuum Mechanics, Proceedings of a Symposium Held in Honour of Henri Cabannes*, pages 19–31, Berlin, 1990. Springer.

44. Y. Sone. *Kinetic Theory and Fluid Dynamics*. Birkhäuser, Boston, 2002.

45. G. Strang. Accurate partial differential methods II. Non-linear problems. *Numer. Math.*, 6:37–46, 1964.

46. B. Wetton. Analysis of the spatial error for a class of finite difference methods for viscous incompressible flow. *SIAM J. Num. Anal.*, 34:723–755, 1997.

47. D. Yu, R. Mei, L.-S. Luo, and W. Shyy. Viscous flow computations with the method of lattice Boltzmann equation. *Prog. Aerospace Sci.*, 39:329–367, 2003.